Appendix A (page 1 of 2)

```
                    10        20        30        40        50        60
          ........|.........|.........|.........|.........|.........|.........   Consensus #1
   1      RPFHFINQTEPLVTHTQQPPSPAPGPASQ-GQRQGNTLLSPTPTPAVILVNPQRAPPVLP   SEQIDNO4
   1      ----MIGSVKRPVVSCVLPEFDFTESTGLGKKSSSVKLPVNFG------AFG            GI 2832300
   1      ----MIAAGAKSLL-----------------GLSMASPK-------G---IFD          GI 1076283
   1      MA----                                                          GI 3529

                    70        80        90       100       110       120
          ........|.........|.........|.........|.........|.........|.........   Consensus #1
                                               TNI.WH........R.....Q.GC..W.TGLS.SGK
  60      GLTPSDAPLPALVIHGLTPRSSHSSAGLASDSGRREGEGRGARTHCHRGIGRWVRRRRN    SEQIDNO4
  43      SGG--GEVKLGFLAPIKATEGSKTSS--FQVNGKVDNFRHLQPSDCNS----            GI 2832300
  23      SNSMSNSRSVVVMRACVSMDGSQTLS--HNKNGSIPEVKSI----                  GI 1076283
   3                                                                      GI 3529

                   130       140       150       160       170       180
          ........|.........|.........|.........|.........|.........|.........   Consensus #1
                                              R.....Q.GC..W.TGLS.SGK
 120      GAAPGEAPHSPVKEKPVMSNIGKSTNILWHNCLIGQSDRQKLLGQKGCVVWITGLSGSGK   SEQIDNO4
  89      DSSLNNCNGFPGKKILQTTIVGNSTNILWHKCAVEKSERQEPLQQRGCVIWITGLSGSGK   GI 2832300
  62      ----NGHTGQKQGPLSTVGNSTNIKWHECSVEKVDRQRLLDQKGCVIWVTGLSGSGK      GI 1076283
   3      ----TNIETMHIP-NLTYDERKALRKQDGCTIWLTGLSASGK                     GI 3529
```

P-loop

Appendix A (page 2 of 2)

P-loop continued

```
                                                                        Consensus #1
        ST.ACAL.L......Y.LDGDN.R.GLN.DL.F...DR.ENIRR..EV.KLFAD...
          190       200       210       220       230       240
180     STLACALSRELHCRGHLTVLDGDNLRHGLNRDLSFKABDRAENIRVGEVAKLFADAGV   SEQIDNO4
149     STLACALSRGIHAKGKITYTLDGDNVFHGLNSDLSFKAEDRAENIRIGEVAKLFADAGV   GI 2832300
115     STLACALNGMLYQKGKLCILLDGDNVTHGLNRDLSPKAEDRAENIRVGEVAKLFADAGI   GI 1076283
38      STIACALEQLLQKNLSAVRLDGDNIRFGLNKDLGESEKDRNENIRISEVSKLFADSCA    GI 3529

                                                                        Consensus #1
        I.I.S.ISPYR...D..R.L......F.E.F.D.PL...E.RDPKGLYK.AR.G.IK.F
          250       260       270       280       290       300
240     CIASILISPYRIDRDACRALUPHSN--FIEVFIIDLPLIKICEAIRDPKGLVYKILARTGKIKGIF  SEQIDNO4
209     CIASILTSPYRIKPPDAQRSLUBGD--FIELEVIFMDVPLIKVIGEAIRDPKGLIMKILARAGKIKGIF GI 2832300
175     CIASILISPYRTDRDACRSLUBBGD--FVELEMDVPLISVICEAIRDPKGLVYKILARAGKIKGIF  GI 1076283
98      SITSFISPYRIVDRDRAREIHKKBAGLKFEIFVDVPLIEMAEQRDPKGLYKARBGVIKIEIF      GI 3529

                                                                        Consensus #1
        TGI..PYE.P....E.............YL.........
          310       320       330       340       350
298     TGIDDPVEPPINGELVIK---MKDEECPSPKAMAKQVLCYLEEENGYLQA                 SEQIDNO4
267     TGIDDPYEPPLUKSEIVIH--QKLGMCDSPCDLADTVISLEENGVLKA                   GI 2832300
233     TGIDDPVEPPLINCELISLG--REGG--TSPIEMAEKVVGYLDNKGYLQA                 GI 1076283
158     TGISAPYEAPKAPELHURTDQKTVEECAT----TIYEVLISEKIIRKHL                  GI 3529
```

Consensus 'Consensus #1': When all match the residue of the Consensus show the residue of the Consensus, otherwise show '.'.

Decoration 'Decoration #1': Shade (with black at 40% fill) residues that match the Consensus exactly.

```
                    10        20        30        40
1   RPPFHFINQIEPLMIHIQQPPSPAPGPPASCGQRQGNILISP   SEQ ID NO4.pro
1   MAS------------------------------------LPV   p0016ctscj40rb.pro
1   MA-------------------------------------     NCBI GI 3529 (Accession CAA46252).pro

                    50        60        70        80
41  IPILAMILVNPQRAPPLPGLIPSDAPLPALVIHGLTLPRS    SEQ ID NO4.pro
7   PHTLP------RIVSPAIVGAARGRAAV------------RV   p0016ctscj40rb.pro
3   -----------------------------------------   NCBI GI 3529 (Accession CAA46252).pro

                    90       100       110       120
81  SHSSAGIASDSGKREGEGRGAR HCHRGLGRMVRRRRNG      SEQ ID NO4.pro
30  RTATATALGGGCG---GGGGMEQR------------        p0016ctscj40rb.pro
3   -----------------------------------------   NCBI GI 3529 (Accession CAA46252).pro

                   130       140       150       160
121 AAAPGEAPHSPVKEKPVMSNIGKSTNILWHNCLIGQSDRQK    SEQ ID NO4.pro
50  --HGDAPHSPVKEKPVMSNIGKSTNILWHNCLIGQSDRQK    p0016ctscj40rb.pro
3   -----------------TNLTIWHPNLTYD-ERKA         NCBI GI 3529 (Accession CAA46252).pro

                   170       180       190       200
161 LLGQKGCVWITGISGSGKSTLACALSRELHCRGHITVVL     SEQ ID NO4.pro
88  LLGQKGCVWITGISGSGKSTLACALSRELHCRGHITVVL     p0016ctscj40rb.pro
19  LRKQDCCTIWLTGLSASGKSHLACALEQLLQKNLSAYRL     NCBI GI 3529 (Accession CAA46252).pro
```

Arrow indicates amino-acid change due to frameshift

1

Appendix B (page 2 of 2)

```
              210       220       230       240
201  DGDNLRHGLNRDISFKAEDRAENIRRVGEVAKLFADAGVL   SEQ ID NO4.pro
128  DGDNLRHGLNRDISFKAEDRAENIRRVGEVAKLFADAGVL   p0016ctscj40rb.pro
59   DGDNIRFGLNKDLGESEKDRNENIRRISEVSKLFADSCAI   NCBI GI 3529 (Accession CAA46252).pro

              250       260       270       280
241  GIASLISPYRRDRDACRALLPHS--NFIEVFIDLPLKICE   SEQ ID NO4.pro
168  GIASLISPYRRDRDACRALLPHS--NFIEVFIDLPLKICE   p0016ctscj40rb.pro
99   SITSFISPYRVDRDRARELHKEAGLKFLEITFVDVPLEVAE  NCBI GI 3529 (Accession CAA46252).pro

              290       300       310       320
279  ARDPKGLYKLARTGKIKGFTGIDDPYEPPINGELVIKMKD   SEQ ID NO4.pro
206  ARDPKGLYKLARTGKIKGFTGIDDPYEPPINGELVIKMKD   p0016ctscj40rb.pro
139  QRDPKGLYKKAREGVIKEFTGISAPVEAPKAPELHLRTDQ   NCBI GI 3529 (Accession CAA46252).pro

              330       340       350
319  ---EECPSPKAMAKQVLCYLEENGYL--QA             SEQ ID NO4.pro
246  ---GECPSPKAMAKQVLCYLEENGYL--QA             p0016ctscj40rb.pro
179  KTVBECATI-----IYEYDISEKIIRKHL              NCBI GI 3529 (Accession CAA46252).pro
```

Shade (with black at 40% fill) residues that match SEQ ID NO4.pro exactly.

2

Appendix C (page 1 of 5)

```
          10        20        30        40        50        60
  1  - - - - - - - - - - - - - - - - - GCGTCCG - - - - TTTCATTTCATCAATCA   SEQ ID NO3.seq
  1  CACCGCCGACCCAGAGACGCTGAGACGCATCCCACATCCACGCATTTCATTTCATCAATCA         p0016ctscj40rb.seq

          70        80        90        100       110       120
 25  AACAGAACCTTCTGGTCACACACGCAGCAACCACCGAGCCCCGGCCGCCCAGCCAG              SEQ ID NO3.seq
 61  AACAGAACCTCTGGTCACACA - - CGGCAACCACCGAGCCCCGGCCGCCCAGCCAG            p0016ctscj40rb.seq

          130       140       150       160       170       180
 85  CCAGGGGCAACGGCCAAGGCCAACACCCTTCCTCAGCGCCGACGCGCTCGCCGTCATCCT          SEQ ID NO3.seq
119  CCAGGGGCCAACGGCCAAGGCCAACACCCTTCCTCAGCCGACGCCGAGCGCTCGCCGTCATCCT      p0016ctscj40rb.seq

          190       200       210       220       230       240
145  CGTAAATCCACAGCGCGCGCTTCCGTCCTGCCCAGGCCTCACCCCTAGCGATGCGCCACT          SEQ ID NO3.seq
179  CGTAAATCCACAGCGCGCGCCTTCCGTCCTCCCAGGCCTCACCCCTAGCGATGCGCCACT          p0016ctscj40rb.seq

          250       260       270       280       290       300
205  CCCGGCGCTTCGTGATCCATGGCCTCACTCCCGTTCCTCACACTCTTCCGCGGTCTCGC          SEQ ID NO3.seq
239  CCCGGCGCTCGTGATCCATGGCCTCACTCCCGTTCCTCACACTCTTCGCGGGTCTCGC            p0016ctscj40rb.seq

          310       320       330       340       350       360
265  CAGTGATAGTTGGCCGCCCGGAGGGGGACTGCCACCGCGGTACGCACTGCCACCGCGCGG         SEQ ID NO3.seq
299  CAGCGATAGTGGGGCCCGGGAGGGGGGACTGCGGTACGCACTGCCACCGCGCGG               p0016ctscj40rb.seq
```

Appendix C (page 2 of 5)

missing nucleotide causing frameshift


```
                  370       380       390       400       410       420
325  CATTGGGCGGTGGGTGCCGGCGGCGGCGGCGGGCGCGGCGAATGGAGCAGGCCC-CGGGGAGGCTCCCCGC  SEQ ID NO3.seq
359  CATTGGGCGGTGGGTGCCGGCGGCGGCGGCGGGCGCGGCGAATGGAGCAGGCCAGCGGGGATGCCCCGG   p0016ctscj40rb.seq

                  430       440       450       460       470       480
384  ACAGCCCAGTGAAGGAGAAGGCCTGTAATGTCGAACATTGCCGAACTAATATTTTAT  SEQ ID NO3.seq
419  ACAGCCCAGTCAAGGAGAAGCCCTCTAATGTCAAACATTGCAAATCCGACTAATATTTAT  p0016ctscj40rb.seq

                  490       500       510       520       530       540
444  GGCACAATTGCTTGATTGGACAATCTGATAGACAGAAATTGCTGGGACAAAAAGGCTGTG  SEQ ID NO3.seq
479  GGCACAATTGCTTGATTGGACAATCTGATAGACAGAAATTGCTGGGACAAAAAGGCTGTG  p0016ctscj40rb.seq

                  550       560       570       580       590       600
504  TCGTATGGATAACAGGACTCAGTGGTTCAGGGAAAAGTACTTCTTGCATGTGCACTGAGTC  SEQ ID NO3.seq
539  TCGTATGGATAACAGGACTCAGTGGTTCAGGGAAAAGTACTTCTTGCATGTGCACTGAGTC  p0016ctscj40rb.seq

                  610       620       630       640       650       660
564  GTGAGTTGCATTGCAGAGAGGCCACCTCACGTATGTACTTGATGGTGACAACCTTCAGACATTG  SEQ ID NO3.seq
599  GTGAGTTGCATTGCAGAGAGGCCACCTCACGTATGTACTTGATGTGACGACAACCTTCAGACATTC  p0016ctscj40rb.seq

                  670       680       690       700       710       720
624  GCCCTAAATAGAGAGATTTAAGCTTTAAGGCAGAAGAGACCCGTGCAGAAATATACGAAGAGTTG  SEQ ID NO3.seq
659  GCCCTAAATAGAGAGATTTAAGCTTTAAGGCAGAAGAGACCCGTGCAGAAATATATACGAAGAGTTC  p0016ctscj40rb.seq
```

Appendix C (page 3 of 5)

```
                730       740       750       760       770       780
684  GTTGAAGTGGCAAAGCTTTTTGCTGATGCTGGTCATTGCATTGCTAGCTTGATATCTC    SEQ ID NO3.seq
719  GTTGAAGTGGCCAAAGCTTTTTCGCTGATGCTGGTGTCATATGCTAGCTTGATATCTC    p0016ctscj40rb.seq

                790       800       810       820       830       840
744  CATACAGGAGAGATCGTGGATGCCATGCCGTGCTCTTACTTCCACATTGTAACTTTATTGAAG   SEQ ID NO3.seq
779  CATACAGGAGAGATCGTGATGCATGCCGTGCTCTTACTTCCACATTCTAACTTTATTGAAG    p0016ctscj40rb.seq

                850       860       870       880       890       900
804  TATTTATTGATTTGCCCCTAAAAATTTGTGAAGCTCGTGATCCTAAAGGCCTATACAAGC    SEQ ID NO3.seq
839  TATTTATTGATTTGCCCCTAAAAATTTGTGAAGCTCGTGATCCTAAAGGCCTATACAAGC    p0016ctscj40rb.seq

                910       920       930       940       950       960
864  TTGCACGTACAGGAAAGATTAAAGGTTTCACTTGAATTGATGATCCATACGAACCACCAA    SEQ ID NO3.seq
899  TTGCACGTACAGGAAAGATTAAAGGTTTCACTTGAATTGATGATCCATACGAACCACCAA    p0016ctscj40rb.seq

                970       980       990       1000      1010      1020
924  TTAATGGTGAGATAGTAATTAAGATGAAAGATGACGAATTGCCCTTCACCCAAAGCAATGG   SEQ ID NO3.seq
959  TTAATGGTGAGATAGTAATTAAGATGAAAGATGGGGAAATGCCCTTCACCCAAAGCAATGG   p0016ctscj40rb.seq

                1030      1040      1050      1060      1070      1080
984  CCAAGCAAGTTCTATGCTACCTTGAAGAAAACGGATATTTGCAAGCCTAGTATATGTATT    SEQ ID NO3.seq
1019 CCAAGCAAGTTCTACCTTGAAGAACGAACCGGATATTTGCAAGCCTTAGCATATGTATT    p0016ctscj40rb.seq
```

Appendix C (page 4 of 5)

```
                    1090      1100      1110      1120      1130      1140
1044   TTGAGAAGATTGATTCTTGTGTGTGTCCATTACTTGTTGCACACAATAAGATCTGTTG   SEQ ID NO3.seq
1079   TTGAGAAGA--GATCTGATTCTTGTGTGTGTCCATTACTTGTTGCACACAATACGATCTGTTG   p0016ctscj40rb.seq

                    1150      1160      1170      1180      1190      1200
1104   TTGGTCACATGAATAAAAGGCATCAACATGTAGGAAGTAACAGAAGGTACGGTTCATTCA   SEQ ID NO3.seq
1137   TTGGTCACATGAATAAAAGCCCATCAACACGTAGGAAGTAACAGAAGGTACGGTTCATTCA   p0016ctscj40rb.seq

                    1210      1220      1230      1240      1250      1260
1164   GAAACGGATAT-------GGATTCATTCGTTT-------CATTGTTGATGATATTTGTTTCG   SEQ ID NO3.seq
1197   GAAACGGATATAGAAACGGATATGGATTCATTCGTTTCATTGTTGATGATATTTGTTTCG   p0016ctscj40rb.seq

                    1270      1280      1290      1300      1310      1320
1189   ------------------------------------------------------------   SEQ ID NO3.seq
1257   CGTGTATTTTGCCTGCATAGCTGCGATTCATTCATCTGCATCAGCAATTCAGGATGCATTCGGT   p0016ctscj40rb.seq

                    1330      1340      1350      1360      1370      1380
1189   ------------------------------------------------------------   SEQ ID NO3.seq
1317   TAACTCGCGTTGACCGTTCGCGCGTCAAATTGGGTAGTTGTTCTGTGCTTGCGAGCTGGGTT   p0016ctscj40rb.seq

                    1390      1400      1410      1420      1430      1440
1189   ------------------------------------------------------------   SEQ ID NO3.seq
1377   CGCTGTTGGCAATGTATTTGTTACAAGTTAATACGGACAAATGTGTAATTTGTGTATCA   p0016ctscj40rb.seq
```

Appendix C (page 5 of 5)

```
              1450      1460      1470      1480      1490
1189          -------------AAAAAAAAAAAAAAAAAAA--AAAAAAAAAA--AAAAAAAAAA
1437          CTTTTTTCCTCTTGGAATAAAGGCGAGGAAACAAAAAACTTAAAAAAAAA
```

SEQ ID NO3.seq
p0016ctscj40rb.seq

Shade (with black at 40% fill) residues that match SEQ ID NO3.seq exactly.

Deletion and Site-directed Mutagenesis of the ATP-binding Motif (P-loop) in the Bifunctional Murine Atp-Sulfurylase/Adenosine 5'-Phosphosulfate Kinase Enzyme*

Andrea T. Deyrup‡, Srinivasan Krishnan‡, Brian N. Cockburn§, and Nancy B. Schwartz¶‖

From the Departments of ‡Pediatrics, ¶Biochemistry and Molecular Biology and §Howard Hughes Medical Institute, The University of Chicago, Chicago, Illinois 60637

The P-loop is a common motif found in ATP- and GTP-binding proteins. The recently cloned murine ATP-sulfurylase/adenosine 5'-phosphosulfate (APS) kinase contains a P-loop (residues 59–66) in the APS kinase portion of the bifunctional protein. A series of enzymatic assays covering the multiplicity of functions of this unique protein (reverse ATP-sulfurylase, APS kinase, and an overall assay) were used to determine the effect of deleting or altering specific residues constituting this motif. In addition to the full-length cDNA construct (1MSK), two deletion mutants that progressively shortened the N terminus by 34 amino acids (2MSK) and 70 amino acids (3MSK) were designed to examine the effects of translation initiation before (2MSK) and after (3MSK) the P-loop. The 2MSK protein possessed sulfurylase and kinase activity equivalent to the full-length construct, but 3MSK exhibited no kinase activity and reduced sulfurylase activity. In light of the evident importance of this motif, a number of site-directed mutants were designed to investigate the contribution of key residues. Mutation of a highly conserved lysine in the P-loop to alanine (K65A) or arginine (K65R) or the following threonine (T66A) to alanine ablated APS kinase activity while leaving ATP-sulfurylase activity intact. Three mutations (G59A, G62A, and G64A) addressed the role of the conserved glycines as follows: G64A showed diminished APS kinase activity only, whereas G62A had no effect on either activity. G59A caused a significant decrease in ATP-sulfurylase activity without effect on APS kinase activity. A series of highly conserved flanking cysteines (Cys-53, Cys-77, and Cys-83) were mutated to alanine, but none of these mutations showed any effect on either enzyme activity.

The P-loop motif is a highly conserved feature of ATP- and GTP-binding proteins where it has been implicated in cleavage of the β-γ-phosphate bond of the NTP (1). Also known as the Walker type A motif, the consensus sequence has been variously described as $(G/A)XXXXGK(T/S)$ (2), $GXXGXXK$ (3), $GXXXXGKS$ (4), and $GXXGXGKS$ (5). This flexible motif generally joins a β-strand and an α-helix to form a pocket into which the phosphate groups can insert. Whereas the N-terminal glycine and C-terminal lysine are absolutely conserved, there is some variability permitted in the intervening amino acids. The lysine side chain has been implicated in hydrogen bonding to the γ-phosphate as demonstrated by x-ray analysis of skeletal myosin bound to an ATP analog (MgADP and beryllium fluoride) (6–8). There is often a serine or threonine following the lysine which provides a hydroxyl group to bind the divalent cation associated with the bound nucleotide (1).

Despite the importance of the terminal lysine, a conservative change to arginine has been shown in some instances to allow attenuated function. Following arginine substitution for the conserved P-loop lysine, the PrtD integral membrane ATP-binding cassette component of the Erwinia chrysanthemi metalloprotease secretion system demonstrated a 10-fold decrease in ATPase activity (9). Similarly, the VirB11 protein of Agrobacterium tumefaciens which also possesses ATPase activity and a Walker consensus sequence is able to mediate DNA transfer with only slight perturbation following a lysine to arginine mutation (10). A nonconservative switch to alanine, however, prevents DNA transfer from the host cell to other plant cells. A conflicting report by Driscoll et al. (3) demonstrated that the nonconserved lysine to alanine substitution in guinea pig estrogen sulfotransferase had no effect on the K_m of the enzyme, suggesting that there is some flexibility in residue requirements.

Another enzyme system in which both ATP and PAPS[1] binding are critical is the sulfate activation pathway, consisting of an ATP-sulfurylase (ATP:sulfate adenylyltransferase, EC 2.7.7.4) reaction that catalyzes the addition of inorganic sulfate to ATP to form APS, followed by an APS kinase (ATP:adenylylsulfate 3'-phosphotransferase, EC 2.7.1.25) reaction which transfers phosphate from ATP to APS to form PAPS (see Reaction 1).

$$ATP + SO_4^{-2} \rightarrow APS + PP_i$$

$$APS + ATP \rightarrow ADP + PAPS$$
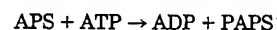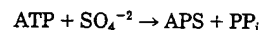
REACTION 1

Since PAPS is the sole source of donor sulfate for all sulfoconjugation reactions in higher organisms, the importance of the sulfate activating enzymes cannot be overstated. We recently cloned the murine ATP-sulfurylase/APS kinase (PAPS synthetase) from brain and showed it to be a fused bifunctional protein through its sequence homology to separate plant and fungal sulfurylases and kinases and by assays of the protein expressed in COS-1 cells (11). The organization of the fused

‖ To whom correspondence should be addressed: The University of Chicago, Dept. of Pediatrics, MC5058, 5841 S. Maryland Ave., Chicago, IL 60637. Tel.: 773-702-9355; Fax: 773-702-9234; E-mail: n-schwartz@uchicago.edu.

[1] The abbreviations used are: PAPS, 3'-phosphate 5'-phosphosulfate; APS, adenosine 5'-phosphosulfate; PCR, polymerase chain reaction; PAGE, polyacrylamide electrophoresis.
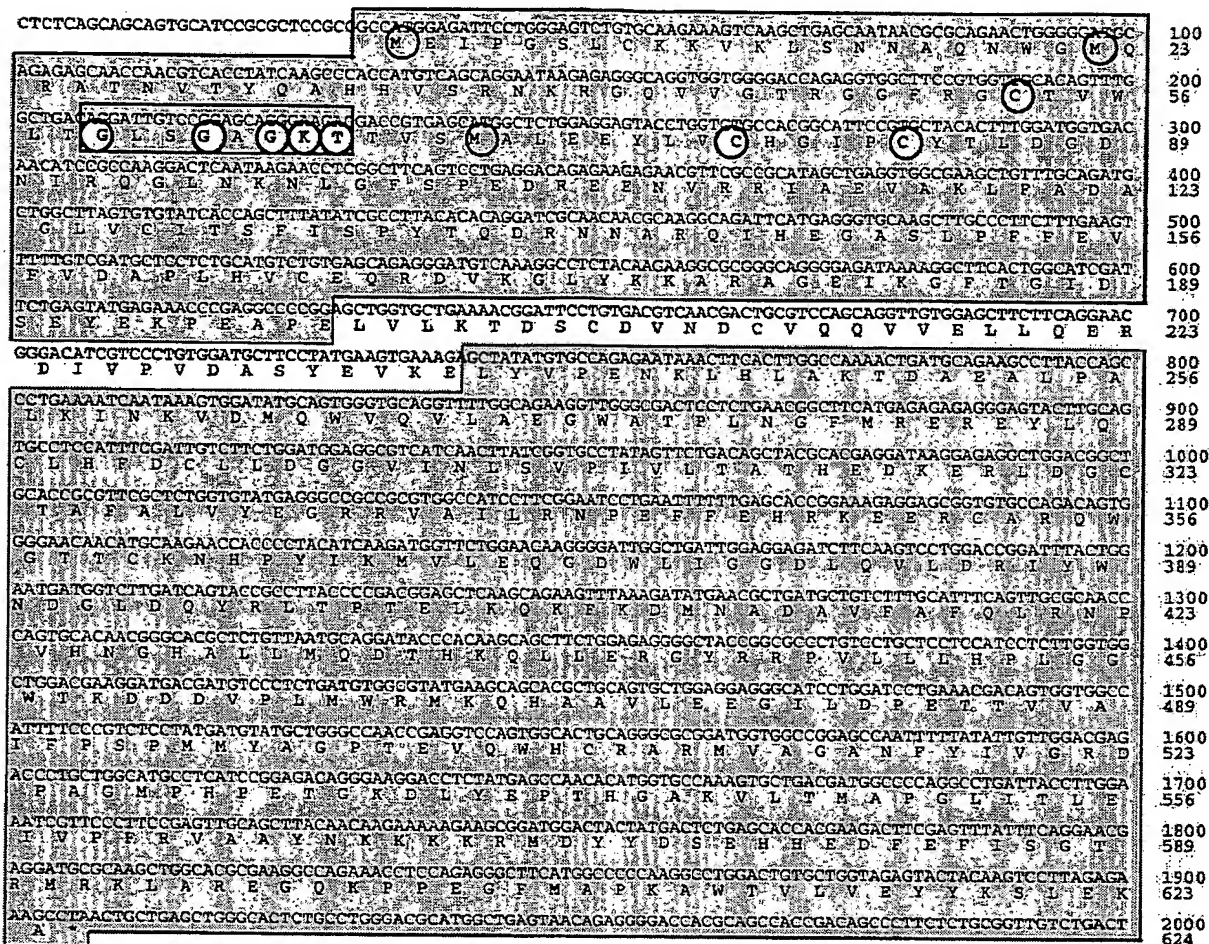
FIG. 1. **Amino acid and nucleotide sequence of the murine ATP-sulfurylase/APS kinase.** The APS kinase domain (*shaded*) extends from residues 1 to 199, followed by the 37-residue linker region and the ATP-sulfurylase domain (*shaded*) which extends from 237 to 624. The P-loop motif is *boxed*, and the modified residues are *circled in white*, and translation initiation methionine of deletion constructs are *circled*.

enzyme includes an APS kinase-homologous domain toward the N terminus (Fig. 1) and an ATP-sulfurylase-homologous domain toward the C terminus. A P-loop motif, GLSGAGKT, is found in the APS kinase portion of the protein from residues 59 to 66. Furthermore, there are three invariant cysteines that flank this motif, cysteine 53 which is upstream from the P-loop and cysteines 78 and 83 which are downstream. Although disulfide bonds have not been previously associated with the P-loop motif, it is possible that in this enzyme they confer structural stability.

Our recent cloning and expression of the murine sulfurylase/kinase (11) provides an opportunity to address specific questions regarding the molecular details of substrate binding to the bifunctional enzyme as well as the relationship of the two active centers in the fused protein. Our initial studies have focused on the P-loop domain, shown to be critical to many enzymatic activities that bind ATP. Here we report the expression of the bifunctional murine brain ATP-sulfurylase/APS kinase in a bacterial host and the effects of deletion or site-specific mutation of essential P-loop residues on the multiple catalytic functions of this enzyme, as assessed by three independent assays as follows: ATP-sulfurylase activity, APS kinase activity, and the overall PAPS synthetase activity. This constitutes the first study that systematically mutated every conserved P-loop residue; the data indicate which of the eight positions mutations can be tolerated and in some cases the chemical nature of amino acid side chain allowed.

EXPERIMENTAL PROCEDURES

Construction of pET-15b/1MSK—The murine brain ATP-sulfurylase/APS kinase coding sequence was obtained from reverse transcriptase-PCR of RNA isolated from 2-day-old C57B mouse brain using the sense primer NdeI N1 = nucleotides 1–20 (5'-GGAATTCCATATG-GAGATTCCTGGGAGTCTG-3') which included the initiation methionine, and the complementary strand primer XhoI N3 = nucleotides 1906 to 1886 (5'-GCTCTAGACTCGAGTTAGGCTTTCTCTAAGG-3'). Each primer included a 5' restriction site to facilitate insertion into the expression vector. Following digestion with NdeI and XhoI, the 1.9-kilobase coding sequence, designated 1MSK, was ligated into an NdeI/XhoI-digested Novagen pET-15b expression vector plasmid and transformed into Invitrogen Top10F' bacterial cells. Positive clones were identified by both restriction mapping and DNA sequencing of the entire insert.

Site-directed Mutagenesis—The pET-15b/1MSK construct was used as the template DNA in all mutagenic PCR reactions. Mutations were produced by 2-step, four primer PCRs in which the N-terminal and C-terminal oligonucleotide primers were identical to those used to generate the pET-15b/1MSK insert (12). Amino acid substitutions are listed in Table I. Briefly, two separate amplification reactions (one using NdeI N1 and the mutant antisense primer and the other using the mutant sense primer and XhoI N3) were done simultaneously for each mutant construct. The two reaction products were electrophoresed on a 1% agarose TAE gel, and the product DNA bands were excised, pooled, and purified using the Qiagen Qiaquick gel extraction kit. This purified DNA was used as the template DNA for a second PCR amplification using the NdeI N1 and XhoI N3 primers. The resulting 1.9-kilobase band was gel-purified and digested with NdeI and XhoI prior to ligation into the NdeI and XhoI sites of pET-15b. The desired ligation products were cloned first into Top10f' cells and subsequently into BL21 (DE3)

Mutational Analysis of P-loop in ATP-Sulfurylase/APS Kinase

TABLE I

P-loop mutant constructs

Amino acid sequences are given for residues 59–66 of murine ATP sulfurylase/APS kinase.

Construct	Sequence
Wild type	GLSGAGKT
G59A	ALSGAGKT
G62A	GLSAAGKT
G64A	GLSGAAKT
K65A	GLSGAGAT
K65R	GLSGAGRT
T66A	GLSGAGKA

for protein expression.

DNA Sequencing—All oligonucleotide primers were purchased from the University of Chicago oligonucleotide core facility. Manual dideoxynucleotide DNA sequencing was performed according to the protocol of the Life Technologies, Inc. T7 polymerase Quick Denature kit using α-^{35}S-dATP from NEN Life Science Products. Approximately 1 μg of closed circular plasmid DNA was denatured in the presence of 25 pmol of sequencing primer. Extension times varied between 10 and 15 min at which point the reaction was terminated. All samples were heated to 70 °C prior to loading onto a 6% acrylamide TBE gel. Dried gels were exposed to Kodak Biomax MR single emulsion x-ray film overnight, and the film was developed the following day. Some automated DNA sequencing was done using the Dye Terminator Cycle Sequencing Ready Reaction Kit from Perkin-Elmer and an ABI PRISM 377 DNA sequencer (Perkin-Elmer).

Polymerase Chain Reaction (PCR)—All PCR amplifications were performed in a Perkin-Elmer GeneAmp 2400 thermal cycler using *Taq* polymerase from Perkin-Elmer. Standard cycling parameters included a 1–5-min preincubation at 94 °C followed by 20–30 cycles of 1 min at 94 °C, 1 min at 60 °C, and 1 min at 72 °C. Following the cycling phase, there was a final extension for 10 min at 72 °C.

Protein Expression—The Novagen pET-15b system was chosen for bacterial expression of the cloned murine brain bifunctional enzyme. All DNA fragments to be expressed were inserted into the NdeI/XhoI doubly-digested plasmid, and all clones were sequenced in their entirety before transformation into BL21 DE3 cells by the CaCl$_2$ method. A single colony was used to inoculate an LB/ampicillin liquid culture which was then placed on a shaker at 37 °C. Growth was continued to an A_{600} of 0.4–1.0 and then the culture was centrifuged, and the cells were resuspended in LB/ampicillin and stored overnight at 4 °C. This suspension culture was subsequently used to inoculate a second, larger LB/ampicillin liquid culture which was grown with shaking at 37 °C for approximately 4 h; then cDNA expression was induced with 0.1 M isopropyl-thio-β-D-galactoside during an additional 3½-h incubation. The cultures were centrifuged at 9000 × g, and the pellet was sonicated in IMAC 5 buffer (5 mM imidazole, 50 mM Tris, pH 7.9). Following removal of cellular debris by ultracentrifugation at 15,000 × g, the supernatant was diluted 1:2 in IMAC 5 sonication buffer.

Protein Purification—To purify the expressed protein, the His-Bind resin and buffer kit from Novagen was used following the supplier's protocol. Briefly, the resin was washed with distilled H$_2$0 to remove ethanol from the storage solution, charged with 100 mM NiSO$_4$, and then equilibrated in sonication buffer. Approximately 8 ml of crude supernatant was loaded onto the 1-ml column in a 1:1 dilution with sonication buffer and incubated at 4 °C for 20 min with intermittent mixing. Following incubation, the flow-through was collected, and the column was washed with 30 mM imidazole to remove the majority of nonspecifically bound bacterial proteins, after which the expressed protein was eluted with 400 mM imidazole. The purified protein was dialyzed into phosphate buffer (25 mM NaH$_2$PO$_4$-K$_2$HPO$_4$, pH 7.8, 1 mM dithiothreitol, 1 mM EDTA) overnight in preparation for enzymatic assays.

Western Blot Analysis—A nickel nitrilotriacetic acid-alkaline phosphatase conjugate purchased from Qiagen was used to analyze the expressed protein by Western blot. The protein was electrophoresed in a 12% SDS-PAGE, transferred to a nitrocellulose membrane, blocked in 3% bovine serum albumin in TBS (150 mM NaCl, 10 mM Tris-HCl, pH 7.4) buffer overnight, and then washed three times in TBST (500 mM NaCl, 0.05% Tween 20, 20 mM Tris-HCl, pH 7.5) buffer. The blot was incubated with the nitrilotriacetic acid-alkaline phosphatase conjugate at a 1:500 dilution in TBST buffer for 2 h and washed as before. The protein band was visualized by treating the blot with nitro blue tetrazolium/5-bromo-4-chloro-3-indoyl-1-phosphate in a Tris buffer (100 mM

NaCl, 5 mM MgCl$_2$, 100 mM Tris-HCl, pH 9.5) followed by a 10% trichloroacetic acid wash and storage in H$_2$O.

Substrate Analog Binding—Dialdehyde ATP was synthesized from [α-^{32}P]ATP as described (13). Dry dialdehyde ATP was dissolved in 0.33 M MgCl$_2$ and added to purified enzyme in a 1:1 molar ratio. The mixture was incubated for 15 min at 37 °C. The reaction was terminated by adding SDS sample buffer and heating the sample in boiling water for 1 min. The samples were run on 10% SDS-PAGE and the gel dried, exposed for autoradiography overnight, and developed.

Enzyme Assays—The optimal protein concentration for assessing enzymatic activity was found to be between 0.3 and 1.0 μg/ml, depending on the assay. Therefore, following gravity column purification, the protein concentration was determined using the Pierce BCA protein assay and diluted with phosphate buffer to a stock concentration of 20 μg/ml for use in all three assays. All assays were performed at least three times; presented data are representatives of individual results. Negative controls were assayed including vector without insert and no vector (DE3 cells alone); for both cases, counts were routinely less than 10% of those obtained with expressed 1MSK crude extract.

The ATP-sulfurylase assay results in formation of ATP, the reverse of the physiological direction (14), due to the unfavorable K_{eq} of the forward reaction. Standard sulfurylase assays contained 50 mM NaH$_2$PO$_4$-K$_2$HPO$_4$, pH 7.8, 12 mM MgCl$_2$, 0.5 mM dithiothreitol, 5 mM NaF, 0.2 mM Na$_4$P$_2$O$_7$ (containing 6.7 mCi of ^{32}P), 0.1 mM APS, and 50 μl of enzyme preparation in a total volume of 1 ml. The generation of ATP from APS and PP$_i$ is quantified.

The standard kinase assay contained 80 nM [^{35}S]APS, 0.5 mM ATP, pH 7.0, 5 mM MgCl$_2$, 10 mM ammonium sulfate, and 12 μl of enzyme and was brought to a total volume of 25 μl with buffer A (25 mM NaH$_2$PO$_4$-K$_2$HPO$_4$, pH 7.8, 1 mM dithiothreitol, 1 mM EDTA, and 10% glycerol) (15). Conversion of the labeled APS substrate to PAPS is monitored by paper electrophoresis which separates the two charged species.

The standard coupled assay assesses the overall reaction with ATP and sulfate as substrates, measuring the production of APS and PAPS. The 25-μl standard overall reaction volume contained 0.4 mM [^{35}S]H$_2$SO$_4$, 10 mM ATP, 20 mM MgCl$_2$, 22 mM Tris-HCl, pH 8.0, and 15 μl of enzyme preparation (15). This assay is valuable not only as a measure of the ability of the enzyme to synthesize PAPS from ATP and SO$_4^{2-}$ but also as an assay of the forward sulfurylase reaction.

Assays were performed in duplicate, and each experiment was repeated at least three times. Kinetic parameters were obtained as described (14).

RESULTS

Expression of the Murine ATP-Sulfurylase/APS Kinase in Bacteria—Since previous expression studies of the recombinant sulfurylase/kinase enzyme were performed in a eukaryotic expression system (11) where proper folding and modification would be expected to occur normally, the correct expression of the recombinant enzyme, physically and functionally, had to be demonstrated in the newly developed bacterial expression system. Following purification of the soluble fraction on the histidine affinity resin, an expressed protein corresponding to the expected molecular weight was visible on SDS-PAGE (Fig. 2). To ascertain that the affinity purified protein was in fact that protein which was expressed from our construct and not a bacterial contaminant, a Western blot using a nickel-conjugated alkaline phosphatase "antibody" was performed; a single band was visualized corresponding to the expressed product at approximately 70 kDa (Fig. 2). Further confirmation that this protein was the ATP-sulfurylase/APS kinase enzyme was obtained by ^{32}P-radiolabeled substrate analog binding using dialdehyde-ATP (16), which labeled a single band at the same molecular weight (Fig. 2). Finally, the 70-kDa band was absent in extracts from induced cells lacking a plasmid construct. Thus, we verified that the bacterial expression system synthesized a recombinant plasmid-specific protein which could be purified and labeled with ATP as expected (16).

Three assays were routinely used as a measure of enzyme activity to assess the level of expression of each recombinant as well as the function of each mutant as follows: the reverse sulfurylase assay, the forward kinase assay, and the overall
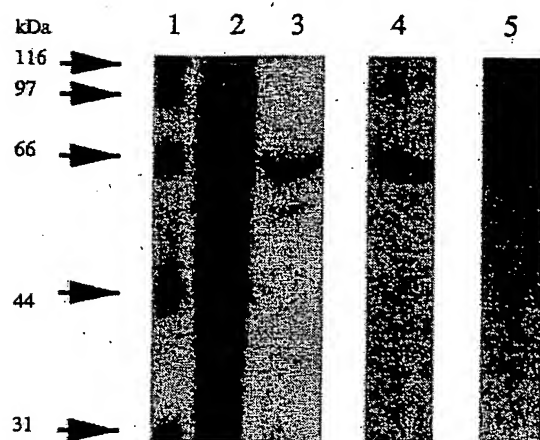
FIG. 2. **Visualization of 1MSK expressed protein.** All samples were electrophoresed in a 10% SDS-acrylamide gel. *Lane 1*, molecular mass standards. *Lane 2*, Crude bacterial extract. *Lane 3*, Coomassie stain of purified 1MSK. *Lane 4*, Western blot analysis of purified 1MSK using a nickel-alkaline phosphatase conjugate. *Lane 5*, O-ATP analog binding to purified 1MSK. Dialdehyde [α-^{32}P]ATP (1.0 ci/mmol) in 50 mM Tris-HCl, pH 8.0, was incubated with purified sulfurylase/kinase enzyme and MgCl$_2$ overnight at 4 °C.

reaction assay. To verify that overexpression of the recombinant protein was accompanied by an increase in enzyme activity, homogenates were first assayed. Soluble extracts obtained from DE3 cells, DE3 cells with empty vector, and DE3 cells transfected with 1MSK exhibited the following activities: sulfurylase, 0.03, 0.05, and 5.13 nmol/min·mg, respectively; and kinase, 0.01, 0.02, and 0.68 pmol/min·mg, respectively. For all subsequent assays the expressed recombinant proteins were purified as described.

Analysis of pET-15b/1MSK and Deletional Mutants—To assess the contribution of the P-loop motif to enzyme function, three cDNA constructs were designed. The first, 1MSK, included the initiator codon ATG at position one. Two further constructs, 2MSK and 3MSK, began at the second and third methionine codons in the cDNA, respectively. Translation at the 2MSK transcript is initiated upstream of the P-loop motif, whereas the 3MSK mutant protein entirely lacks the P-loop. Enzyme activities of the 1MSK and 2MSK constructs were found to be nearly identical in all three assays (Table II); however, the 3MSK construct exhibited decreased reverse sulfurylase activity (66% of wild type) and complete absence of kinase and overall activities.

Analysis of Site-directed Mutants—Although a great deal of experimental work has focused on the P-loop motif in various systems, a comprehensive site-specific analysis of essential residues has not yet been accomplished in any single study reported in the literature. Accordingly, in this study, all of the conserved residues were individually altered, and the effect of each change on sulfurylase/kinase enzyme activities was assessed (Table III and Fig. 3). The lysine residue at the C-terminal end of the P-loop motif has been implicated in NTP binding (1). Substitution of Lys-65 with alanine had some effect on sulfurylase activity (80% residual activity; 20.5 μmol of ATP/min·mg as compared with 24.4 μmol of ATP/min·mg for 1MSK) but almost completely ablated kinase activity (4% residual activity; 6.2 pmol of PAPS/min·mg as compared with 160.8 pmol of PAPS/min·mg). Lysine and alanine differ not only in size and structure but also in charge; therefore, a second, more conservative mutation was engineered to determine if substitution with an arginine would have a less deleterious effect. The K65R mutant restored sulfurylase activity (96% residual activity, 23.3 μmol of ATP/min·mg); however, the kinase was no more active than the K65A mutant (3% residual

TABLE II
Specific activity of deletion mutants

Three constructs, 1MSK, 2MSK, and 3MSK, initiating at the first, second, and third methionines, respectively, were generated. The purified expressed protein was assayed for sulfurylase, kinase, and overall activity. The results had a maximum error of 5% between duplicates of each sample and of 10% between batches of all samples.

Construct	Sulfurylase assay	Kinase assay	Overall assay	
	μmol ATP min^{-1} mg^{-1} (×10^{-1})	pmol PAPS min^{-1} mg^{-1}	nmol APS min^{-1} mg^{-1} (×10^{-1})	nmol PAPS min^{-1} mg^{-1}
1MSK	24.4	160.8	2.4	11.7
2MSK	23.1	157.5	2.5	12.5
3MSK	16.2	1.8	4.7	0.09

TABLE III
Specific activity of site-specific mutants

Nine constructs were designed to examine the P-loop phosphate-binding motif: C53A, G59A, G62A, G64A, K65A, K65R, T66A, C78A, and C83A. The purified expressed products were assayed for sulfurylase, kinase, and overall activity. The results had a maximum error of 5% between duplicates of each sample and of 10% between batches of all samples.

Construct	Sulfurylase assay	Kinase assay	Overall assay	
	μmol ATP min^{-1} mg^{-1} (−10^{-1})	pmol PAPS min^{-1} mg^{-1}	nmol APS min^{-1} mg^{-1} (×10^{-1})	nmol PAPS min^{-1} mg^{-1}
1MSK	24.4	160.8	2.4	11.7
C53A	22.6	178.3	4.2	22.7
G59A	1.9	242.2	0.7	0.6
G62A	23.9	180.1	6.0	7.8
G64A	25.8	10.2	9.9	0.1
K65A	20.5	6.2	6.8	0.1
K65R	23.3	5.3	8.6	0.02
T66A	24.3	25.6	7.9	0.2
C78A	23.5	178.0	2.9	25.6
C83A	22.6	195.8	1.2	10.1

activity; 5.3 pmol of PAPS/min·mg) suggesting that charge preservation alone was insufficient to rescue the altered motif.

The hydroxyl group of the threonine/serine P-loop element is primarily regarded as having a role in anchoring the divalent cation, Mg^{2+}, associated with the bound nucleotide in the sulfurylase/kinase (1). Substitution of an alanine for the threonine would remove this stabilizing group, and in fact, introduction of this mutation (T66A) resulted in a substantial decrease in the ability of the enzyme to catalyze the kinase reaction (16% residual activity; 25.6 pmol of PAPS/min·mg), although to a lesser degree than the Lys-65 mutations. Interestingly, despite the severe effect of all three of these mutations (K65A, K65R, and T66A) on kinase activity, they produced no apparent deficit in sulfurylase activity. These data suggest that the expressed protein is not only in the correct conformation but also that the sulfurylase domain can function independently of the mutated kinase domain, even in the fused enzyme in the reverse direction. The overall reaction, however, was unable to proceed to PAPS formation due to the inability of the mutants to catalyze the kinase reaction, even though the formation of APS was normal (Table III).

The role of providing conformational flexibility has been attributed to the glycine-rich region of the P-loop (1). Accordingly, alanine was substituted for each of the three glycines individually to reduce conformational freedom at these locations. Although the G62A mutant had no effect on sulfurylase or kinase and some effect on overall activity (67% residual activity; 7.78 nmol of PAPS/min·mg), both of the other glycines proved essential for enzyme activity. The G64A substitution was deleterious to kinase activity (6% residual activity; 10.2 pmol of PAPS/min·mg) without affecting sulfurylase activity (105% activity; 2.58 mmol of ATP/min·mg). Interestingly, the N-terminal glycine (Gly-59), which is highly conserved as the
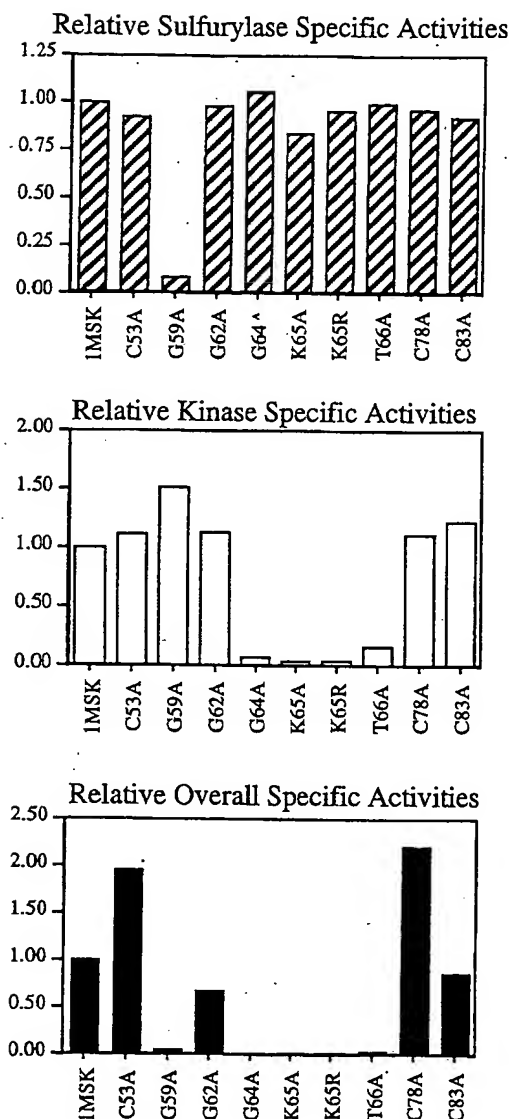
Relative Sulfurylase Specific Activities

Relative Kinase Specific Activities

Relative Overall Specific Activities

FIG. 3. **Relative specific activity of mutant constructs.** Specific activities were normalized to the activity determined for 1MSK in each assay as given in Table III.

initiator of the P-loop sequence, when mutated to an alanine exhibited greatly decreased sulfurylase activity (8% residual activity; 0.19 μmol of ATP/min·mg) and some increase in kinase activity (150% activity; 242.2 pmol of PAPS/min·mg). These findings demonstrate that the kinase domain may be active even though the sulfurylase domain is nonfunctional. Overall activity was compromised in both G59A and G62A mutants since, presumably in the former, no APS was generated internally for the subsequent kinase reaction, whereas in the latter the final phosphorylation step was blocked thereby preventing PAPS formation.

Although disulfide bonds have not been identified in previously analyzed P-loop motifs, the murine ATP-sulfurylase/APS kinase has 21 cysteine residues of which 3 clustered around the P-loop are the most highly conserved in other APS kinases/kinase domains (Cys-53 in *Saccharomyces cerevisiae*, *Arabidopsis thaliana*, mouse, and human; Cys-78 in mouse and human; and Cys-83 in *A. thaliana*, mouse, and human). These three cysteines flank the P-loop with Cys-53 upstream of the motif and Cys-78 and Cys-83 downstream. The possibility therefore exists that disulfide bonds are involved in structural stabilization. Hence, three separate constructs were designed

by substituting alanine for each cysteine individually. None of these mutations appeared to have any detrimental effects on the kinase, sulfurylase, or overall activities (Table III). When the marine worm (*Urechis caupo*) (17) and *Drosophila* sulfurylase/kinase DNA sequences recently became available, it was noted that neither Cys-78 nor Cys-83 were conserved in these species; Cys-78 was replaced by a serine in both cases, and Cys-83 was replaced by a threonine in the worm and by alanine in the fruit fly. The variance among the fused enzymes of non-mammalian species is of particular interest considering their conservation in the more widely divergent subsets described above. This lack of conservation indicates that flexibility exists for these residues.

DISCUSSION

The bifunctional sulfurylase/kinase that we originally purified from rat chondrosarcoma (16, 18, 19) and recently cloned from mouse brain (11) would be expected to require binding sites for at least two molecules of ATP and one molecule of APS/PAPS. The single P-loop motif in the APS kinase domain which has been shown in other proteins to bind ATP, and perhaps PAPS, was therefore targeted for mutagenesis. However, based on the reaction stoichiometry a second nucleotide-binding site may be expected to occur. The P-loop extending from residues 59 to 66 in the murine sulfurylase/kinase fits the Walker type A consensus motif GXXGXGK(T/S). The sequence and location of this motif is highly conserved across the known fused sulfurylase/kinases where it is found from residues 59 to 65 in mouse (11) and human,[2] from residues 44 to 51 in worm (17), and from residues 54 to 61 in fruit fly.[3]

Two deletion mutants were designed to assess the contribution of the P-loop to enzyme activity. The small (34-amino acid) N-terminal deletion of the 2MSK construct did not affect enzyme activity; however, complete deletion of the P-loop in the 3MSK construct not only eliminated kinase activity but also decreased sulfurylase activity. Although the structural consequences of deleting 70 amino acids from the N termini have not been established for this protein, the ability of the 3MSK sulfurylase domain to exhibit significant activity would suggest that the remainder of the fused protein is structurally stable.

To more accurately dissect the contribution of the P-loop motif, a series of site-specific mutants was created and assayed. The observed detrimental effect of the K65A and K65R substitutions (Table II) is well supported in the literature. The conserved lysine has been implicated in hydrogen bonding to the γ-phosphate as discussed previously (6–8). In such a structure, alanine would clearly be unable to compensate for the charged lysine residue. Arginine, although possessing a different structure, is a candidate for providing the necessary charge stabilization. The inability of the arginine substitution to restore activity to the fused sulfurylase/kinase cannot be directly attributed to a defect in hydrogen bonding. The bulky arginine side chain may be sufficient to disrupt the NTP binding pocket or even the entire N-terminal end of the protein, thereby ablating enzyme activity. Logan and Knight (21) also found that arginine could not substitute for the conserved lysine in *Escherichia coli* RecA.

In myosin, EF-Tu, *RAS*, and the G-proteins, the coordination sphere of the magnesium ion includes two oxygen atoms from the β- and γ-phosphates of the bound trinucleotide, the hydroxyl side chain from the threonine or serine at position 8, and two water molecules (1). In the APS kinase reaction the Mg^{2+} associated with the ATP molecule is potentially stabilized by

---

[2] A. Deyrup, S. Krishnan, B. Singh, and N. B. Swartz unpublished observations.

[3] D. Jullien and E. Kas, EMBL accession number Y12861.

the Thr-66 hydroxyl group. Substitution with alanine substantially reduced kinase activity in the fused sulfurylase/kinase which suggests that the position of the magnesium ion in this enzyme may be critical. In addition to lacking non-bonding electrons, however, alanine differs from threonine *vis à vis* molecular volume and polarity. Further dissection of the roles of steric effects could be accomplished through alternative substitutions with valine and serine.

The structural flexibility conferred by the cluster of glycines in the P-loop has been implicated in binding of the nucleotide triphosphate as allowing adjacent amino acids to form backbone hydrogen bonds with the β- and γ-phosphate groups (1). However, changing either the initial (Gly-59) or second glycine (Gly-62) to an alanine did not decrease kinase activity. Substitution of a bulkier residue or proline may prove necessary to disrupt enzyme function. In the case of familial persistent hyperinsulinemic hypoglycemia of infancy, a spontaneous mutation of the second glycine to a valine in the P-loop motif of the sulfonylurea receptor causes the pathological state (22), and therefore, valine would also be a logical choice for further glycine mutagenesis. However, in many ATP-binding proteins, the second glycine of the motif (in our case Gly-62) is not considered a feature of the motif (4, 23). Therefore, the role of the second glycine appears to be highly variable and, furthermore, appears dispensable in the fused sulfurylase/kinase.

In contrast to the G64A mutation in the kinase domain which affects kinase activity, the G59A substitution in the kinase domain completely ablates sulfurylase activity in both directions and thus overall PAPS activity but does not affect the kinase reaction when exogenous APS is supplied. The loss of activity for the G59A mutation is especially surprising considering that, in an early report, Saraste *et al.* (23) found that the first residue of the P-loop could be either an alanine or a glycine (23). An initial alanine is found predominantly among the P-loops of elongation factors and phosphoglycerate kinases as well as in a thymidine kinase (23). However, the inability of an alanine to satisfactorily substitute for this initial glycine has been demonstrated in the *E. coli* RecA protein (21).

The loss of function of the G59A mutant suggests that there may be some interaction between the N- and C-terminal domains of the protein or that the P-loop is folded into close contact with a critical portion of the sulfurylase domain. Models have been proposed for several enzymes in which nucleotide triphosphate binding and hydrolysis control specific conformational changes critical to protein function. Thus the role of the P-loop most likely involves not only the provision of a hydrophobic binding pocket for NTP but also a flexible structure that can undergo a conformational change in response either to substrate binding or an interaction with another protein or domain (24). In turn, the conformational change may control access of subsequent substrates to the active site, modification of binding affinities, or relocation of reactive groups toward the reaction center of the bound substrate. These actions are not mutually exclusive and could be operating to varying degrees or combinations to facilitate catalysis not only at the kinase active site but at the sulfurylase site as well.

Moreover, the mechanistic interdependence, if any, of the two activities has not yet been established for the fused enzyme. Modification of the sole nucleotide-binding site therefore also offered the opportunity to explore the relationship of the two functions. Since Gly-59 appears to play an important role in the interaction between the sulfurylase and kinase domains, the effect of this mutation on sulfurylase activity measured in both the forward and reverse directions indicates that this glycine is involved in stabilizing a structure necessary for nucleotide triphosphate binding, a function common to reactions

in both directions, rather than in SO_4^{2-} binding. This possibility is highlighted by a specific mutation we have made in the sulfurylase domain which affects the forward sulfurylase reaction only with no effect on the reverse reaction, suggesting that this residue participates predominantly in SO_4^{2-} binding.[2] A full understanding of the relationship between the two portions must await a more detailed structural analysis of our mutants, which is beyond the scope of the present study.

The P-loop in the sulfurylase/kinase is particularly interesting considering that in addition to a role in ATP binding, a variation of this motif (G*XX*G*XX*K) has also been implicated in PAPS binding (3, 25). The bifunctional ATP-sulfurylase/APS kinase would be expected to bind two molecules of ATP for each complete enzymatic reaction, as well as one molecule of PAPS; however, only a single P-loop, with all the consensus features, has been identified in the bifunctional enzyme. It is possible, therefore, that there is an additional nucleotide-binding site which is not a P-loop motif or is a more modified version. Additional searches using FINDPATTERNS has confirmed no additional motifs of the form G*XXXXX*K; however, another ATP/GTP binding motif, D*XX*G (26–28), is found starting at residues 169 and 523. The potential contribution of these motifs is under investigation. Alternatively, the single P-loop may be used to bind the ATP required for each reaction. Since rat ATP-sulfurylase/APS kinase employs intermediate channeling to pass the labile APS intermediate from the ATP-sulfurylase active site to the APS kinase active site (29), a possible mechanism to facilitate channeling might involve substrate binding to a single site resulting in a conformational change which serves to bring the subsequent active site into proximity. Because the P-loop is a potential binding site for both ATP (substrate) and PAPS (product), it is a likely candidate for binding one or more of the sulfurylase/kinase reactants and/or products, and further investigation of the roles of the various residues that constitute this important motif is necessary.

In sum, this study constituted a molecular dissection of a putative motif previously considered important in ATP- and PAPS-binding proteins. Our results demonstrate that while the consensus residues Gly-59, Gly-64, Lys-65, and Thr-66 are strictly required, the Gly-62 position can tolerate substitution. Furthermore, we were able to group the sulfurylase/kinase mutants into three general phenotypic categories as follows: those deficient in sulfurylase activity only, kinase activity only, or those that exhibited minimal loss of either activity. In this set of mutants the other potential phenotypic category, *i.e.* normal sulfurylase and kinase individual activities, but reduced overall activity was not observed; however, we have obtained such a mutant from a set of substitutions in the sulfurylase region.[2]

A final point of interest is that in all proteins bearing functional P-loop motifs, this sequence is located near the N terminus of the protein where it forms a loop between a β-strand and an α-helix. This arrangement is maintained in the murine, human, and worm fused sulfurylase/kinase that have a domain organization in which the kinase domain is positioned at the N terminus of the bifunctional enzyme, and the sulfurylase domain is toward the C terminus. This order is the reverse of the gene order in the *E. coli* operon (30) and the *Penicilium chrysogenum* sulfurylase with a fused C-terminal portion similar to kinase sequence (20), which are all structurally ordered as in the reaction sequence. Therefore, placing the kinase at the N terminus in the fused sulfurylase/kinase of higher organisms may allow the same flexible orientation of the P-loop motif seen in other ATP- and GTP-binding proteins. Had the sulfurylase and kinase been fused in the order found in the arrangement of the genomes of lower organisms, the P-loop would be buried in

the sequence and most likely more conformationally constrained.

REFERENCES

1. Smith, C., and Rayment, I. (1996) *Biophys. J.* 70, 1590–1602
2. Walker, J., Saraste, M., Runswick, M., and Gay, N. (1982) *EMBO J.* 1, 945–951
3. Driscoll, W. J., Komatsu, K., and Strott, C. A. (1995) *Proc. Natl. Acad. Sci. U. S. A.* 92, 12328–12332
4. Satishchandran, C., Hickman, Y. N., and Markham, G. D. (1992) *Biochemistry* 31, 11684–11688
5. Thomas, P. M., Wohllk, N., Huang, E., Kuhnle, U., Rabl, W., Gagel, R. F., and Cote, G. J. (1995) *Am. J. Hum. Genet.* 59, 510–518
6. Fisher, A., Smith, C., Thoden, J., Smith, R., Sutoh, K., Holden, H., and Rayment, I. (1995) *Biochemistry* 34, 8960–8972
7. Fisher, A., Smith, C., Thoden, J., Smith, R., Sutoh, K., Holden, H., and Rayment, I. (1995) *Biophys. J.* 68, (Suppl. 4), 19–28
8. Rayment, I., Rypniewski, W., Schmidt-Base, K., Smith, R., Tomchick, D., Benning, M., Winkelmann, D., Wesenberg, G., and Holden, H. (1993) *Science* 261, 50–58
9. Delepelaire, P. (1994) *J. Biol. Chem.* 269, 27952–27957
10. Stephens, K., Roush, C., and Nester, E. (1995) *J. Bacteriol.* 177, 27–36
11. Li, H., Deyrup, A., Mensch, J., Domowicz, M., Konstantinidis, A., and Schwartz, N. B. (1995) *J. Biol. Chem.* 270, 29453–29459
12. Higuchi, R. (1989) in *PCR Technology: Principles and Applications for DNA Amplification* (Erlich, H. A., ed) pp. 61–70, Stockton Press, New York
13. Lowe, P. N., and Beechey, R. P. (1982) *Bioorg. Chem.* 11, 55–71
14. Lyle, S., Geller, D. H., Ng, K., Stanzak, J., Westley, J., and Schwartz, N. B. (1994) *Biochem. J.* 301, 355–359
15. Lyle, S., Geller, D. H., Ng, K., Westley, J., and Schwartz, N. B. (1994) *Biochem. J.* 301, 349–354
16. Lyle, S., Stanzack, J., Ng, K., and Schwartz, N. B. (1994) *Biochemistry* 33, 5920–5925
17. Rosenthal, E., and Leustek, T. (1995) *Gene (Amst.)* 165, 243–248
18. Geller, D., Henry, J. G., Belch, J., and Schwartz, N. B. (1987) *J. Biol. Chem.* 262, 7374–7382
19. Geller, D. H. (1987) *The Sulfate-activating Enzyme of Cartilage Tissue*, Ph.D. thesis, University of Chicago
20. Foster, B. A., Thomas, S. M., Mahr, J. A., Renosto, F., Patel, H. C., and Segel, I. H. (1994) *J. Biol. Chem.* 269, 19777–19786
21. Logan, K., and Knight, K. (1993) *J. Mol. Biol.* 232, 1048–1059
22. Thomas, P., Wohllk, N., Huang, E., Kuhnle, U., Rabi, W., Gagel, R., and Cote, G. (1996) *Am. J. Hum. Genet.* 59, 510–518
23. Saraste, M., Sibbald, P. R., and Wittinghofer, A. (1990) *Trends Biochem. Sci.* 15, 430–434
24. Fry, D. C., Kuby, S. A., and Mildvan, A. S. (1986) *Proc. Natl. Acad. Sci. U. S. A.* 83, 907–911
25. Komatsu, K., Driscoll, W. J., Koh, Y. C., and Strott, C. A. (1994) *Biochem. Biophys. Res. Commun.* 204, 1178–1185
26. Sung, Y.-J., Carter, M., Zhong, J.-M., and Huang, Y.-W. (1995) *Biochemistry* 34, 3470–3477
27. Sage, C. R., Dougherty, C. A., Davis, A. S., Burns, R. G., Wilson, L., and Farrell, K. W. (1995) *Biochemistry* 34, 7409–7419
28. Taylor, G. A., Jeffers, M., Largaespada, D. A., Jenkins, N. A., Copeland, N. G., and Vande-Woude, G. F. (1996) *J. Biol. Chem.* 271, 20399–20405
29. Lyle, S., Ozeran, J. D., Stanzak, J., Westley, J., and Schwartz, N. B. (1994) *Biochemistry* 33, 6822–6827
30. Leyh, T. S., Vogt, T. F., and Suo, Y. (1992) *J. Biol. Chem.* 267, 10405–10410

Characterization of the Phosphorylated Enzyme Intermediate Formed in the Adenosine 5'-Phosphosulfate Kinase Reaction[†]

C. Satishchandran, Yvette N. Hickman, and George D. Markham[*]

Institute for Cancer Research, Fox Chase Cancer Center, 7701 Burholme Avenue, Philadelphia, Pennsylvania 19111

Received July 28, 1992; Revised Manuscript Received September 21, 1992

ABSTRACT: Adenosine 5'-phosphosulfate (APS) kinase (ATP:APS 3'-phosphotransferase) catalyzes the ultimate step in the biosynthesis of 3'-phosphoadenosine 5'-phosphosulfate (PAPS), the primary biological sulfuryl donor. APS kinase from *Escherichia coli* is phosphorylated upon incubation with ATP, yielding a protein that can complete the overall reaction through phosphorylation of APS. Rapid-quench kinetic experiments show that, in the absence of APS, ATP phosphorylates the enzyme with a rate constant of 46 s^{-1}, which is equivalent to the V_{max} for the overall APS kinase reaction. Similar pre-steady-state kinetic measurements show that the rate constant for transfer of the phosphoryl group from E-P to APS is 91 s^{-1}. Thus, the phosphorylated enzyme is kinetically competent to be on the reaction path. In order to elucidate which amino acid residue is phosphorylated, and thus to define the active site region of APS kinase, we have determined the complete sequence of *cys*C, the structural gene for this enzyme in *E. coli*. The coding region contains 603 nucleotides and encodes a protein of 22 321 Da. Near the amino terminus is the sequence [35]GLSGSGKS, which exemplifies a motif known to interact with the β-phosphoryl group of purine nucleotides. The residue that is phosphorylated upon incubation with ATP has been identified as serine-109 on the basis of the amino acid composition of a radiolabeled peptide purified from a proteolytic digest of ^{32}P-labeled enzyme. We have identified a sequence beginning at residue 147 which may reflect a PAPS binding site. This sequence was identified in the carboxy terminal region of 10 reported sequences of proteins of PAPS metabolism.

3'-Phosphoadenosine 5'-phosphosulfate (PAPS)[1] is the major donor of sulfuryl (SO₃) groups in biological systems (Huxtable, 1986; Falany, 1991). The biosynthesis of PAPS from ATP and inorganic sulfate occurs in two steps: first, ATP sulfurylase (ATP:sulfate adenylyltransferase) catalyzes the reaction of ATP and sulfate to yield adenosine 5'-phosphosulfate and pyrophosphate, and second, APS kinase (ATP:APS 3'-phosphotransferase) catalyzes the ATP-dependent phosphorylation of the 3'-hydroxyl of APS (Robbins & Lipman, 1958). Cloning of the structural genes for APS kinase and ATP sulfurylase from *Escherichia coli* has been reported (Leyh et al., 1988). We recently described purification of APS kinase from an overproducing strain of *E. coli* and characterization of the physical and steady-state kinetic properties of the enzyme (Satishchandran & Markham, 1989). Purified APS kinase was found to be phosphorylated upon incubation with ATP at a stoichiometry of one phosphoryl group per subunit (E-P). The phosphoryl group of E-P could be transferred either to APS to yield PAPS or to ADP to form ATP, suggesting that E-P may be an intermediate in the APS kinase reaction. Involvement of a phosphorylated enzyme in the reaction would rationalize the complex steady-state kinetic behavior of the enzyme, which reflects a combination of ping-pong and sequential pathways (Satishchandran & Markham, 1989). Phosphorylated enzyme intermediates are unusual in phosphoryl-transfer reactions where the acceptor is a small

molecule (Knowles, 1980). The only simple kinase reaction which has been shown to proceed through a phosphorylated enzyme intermediate is catalyzed by nucleoside diphosphate kinase, which shows classical ping-pong kinetics with a single substrate binding site for donor and acceptor (Garces & Cleland, 1969). Identification of the amino acid which becomes phosphorylated in *E. coli* APS kinase is of particular interest since the APS kinase from *Penicillium chrysogenum* is not detectably phosphorylated by incubation with ATP (Renosto et al., 1991). Here we report the complete sequence of the *cys*C gene that encodes APS kinase and identification of the phosphorylated residue.[2]

MATERIALS AND METHODS

APS was synthesized and purified as described previously (Baddiley et al., 1957; Yount et al., 1966; Satishchandran & Markham, 1989). APS kinase was purified to electrophoretic homogeneity from the overproducing *E. coli* strain JM83/pTL3/pGP1-2 following the published method; the enzyme concentration was determined using the extinction coefficient of 1.047 $(mg/mL)^{-1}$ cm^{-1} at 280 nm (Satishchandran & Markham, 1989). Other compounds were purchased from commercial sources.

DNA Sequencing. The synthetic oligonucleotides used as primers for DNA sequencing were prepared by Applied Biosystems Instruments at the core facility of the Institute for Cancer Research. Double-stranded plasmid DNA was sequenced using the Sequenase II kit from US Biochemicals following the instructions of the manufacturer. DNA fragments were separated electrophoretically on denaturing polyacrylamide gels prepared with the GIBCO-BRL Sequencing Gel kit. The entire sequence was obtained using both strands of previously reported plasmids as templates.

[*] Corresponding author.

[1] Abbreviations: APS, adenosine 5'-phosphosulfate; E-P, phosphorylated APS kinase; GCG, Genetics Computer Group; HPLC, high-performance liquid chromatography; PAP, 3'-phosphoadenosine 5'-phosphate; PAPS, 3'-phosphoadenosine 5'-phosphosulfate; PEI, polyethyleneimine; TFA, trifluoroacetic acid; TPCK, L-1-tosylamido-2-phenylethyl chloromethyl ketone.

[2] A preliminary report of these studies was presented at the Fourth International Congress of Chemistry in New York, 1991.

DNA Sequence Analysis. Individual sequences were assembled and the final data analyzed using the GCG suite of computer programs (Devereux et al., 1984). The final sequence has been deposited in GenBank as Accession Number M86936. Searches for similar sequences in the computer databases used the FASTA program (Pearson, 1990) with GenBank Release 69.0. In a search for a potential PAPS binding motif, the three available APS kinase sequences [*met*14 of *Saccharomyces cerevisiae* (Korch et al., 1991), *nodQ* of *Rhizobium meliloti* (Schwedock & Long, 1990) and *cysC*], the six published sulfotransferase sequences (Nash et al., 1988; Ozawa et al., 1990; Roche et al., 1991; Ogura et al., 1989; Varin et al., 1991), and a homologous aging-related protein (Chaterjee et al., 1987) were aligned in pairwise fashion using BESTFIT, and then as group using the PILEUP program. The final alignment was displayed using the program MALIGNED (Clark, 1992). The potential motif was tested against the PIR-Protein database Release 30.0 and Swissprot Release 19.0 using the FINDPATTERNS program; all possible residues were allowed at the X positions. In order to identify potential known motifs in APS kinase, the deduced APS kinase sequence was inspected using the program MOTIFS with the ProSite motif database (Release 8.0).

Amino Terminal Protein Sequence. Purified APS kinase (1.5 nmol) was sequenced by Dr. E. Burke on an Applied Biosystems 4778 instrument at the Peptide Sequencing Facility of the Albert Einstein College of Medicine, Bronx, NY.

Identification of the Type of Phosphorylated Residue. ^{31}P NMR spectra were recorded on a Bruker AM–300 spectrometer operating at 121.45 MHz. Samples contained 50 mM Hepes/KOH, pH 8.0 with 10% D_2O for field-frequency locking. Chemical shifts are referenced to 85% phosphoric acid; positive chemical shifts are downfield with respect to the reference.

Identification of the Phosphorylated Peptide. A 10-nmol sample of enzyme was phosphorylated by incubation with 1 mM [γ-^{32}P]ATP (20 mCi/mmol) for 0.5 h at 25 °C in 0.1 mL containing 50 mM Hepes/KOH, 50 mM KCl, and 2 mM $MgCl_2$. After removal of nucleotides by gel filtration on Sephadex G-50 using 50 mM sodium phosphate and 2 mM EDTA, pH 7.8, as the eluant, the phosphorylated enzyme was concentrated using a Amicon Centricon 10 device. The enzyme was treated with 5 μg of staphylococcal protease V8 in 0.1 mL of 50 mM sodium phosphate, 2 mM EDTA, and 0.1 mg/mL TPCK, pH 7.8, for 4 h at 37 °C. Peptides were then separated by reverse-phase HPLC on a Vydac C-18 column (218TP54) attached to a Waters Model 600 instrument. The column was eluted at a flow rate of 1 mL/min with a gradient between water-containing 395 μL/L TFA (solvent A) and acetonitrile-containing 360 μL/L TFA (solvent B). The overall gradient was composed of several linear gradients as described by Jaffe et al. (1992). Elution was monitored at 214 nm. Fractions were collected and radioactivity was determined. The sole radioactive peak eluted 98 mL after injection and corresponded to a peak absorbing at 214 nm which was well resolved from other peaks. The composition of the peptide was determined by Dr. W. Abrams at the Protein Analytical Laboratory of the University of Pennsylvania School of Dental Medicine using a Maxima (c) Dynamic Solutions instrument (Millipore).

Rapid Chemical Quench Kinetic Studies. Rapid-quench experiments used a KinTek RQF-3 quench flow instrument (KinTek Instruments, University Park, PA). The dead time of the instrument was determined to be 2 ms by calibration using the base-catalyzed hydrolysis of benzylidenemalononitrile as described by the instrument manufacturer. To measure the rate of E-P formation, 62.5 μM enzyme was mixed with 0.5 mM [γ-^{32}P]ATP (20 Ci/mmol) (final concentrations) in 50 mM Hepes, 50 mM KCl, 1 mM $MgCl_2$, and 10% glycerol, pH 8.0, at 25 °C. After incubation times varying between 2 and 500 ms, the reactions were terminated by mixing with 10% TCA (final concentration) in 10% glycerol. The quenched reactions were collected in a tube containing 0.1 mg of bovine serum albumin. After incubation on ice for 30 min, the protein precipitate was collected on glass fiber filters (Millipore), the filters were washed extensively with 10% TCA, and the extent of protein phosphorylation was quantified by scintillation counting. In experiments measuring the rate of transfer of the phosphoryl group of E-P to APS, 12.5 μM E-P (prepared as described above) was mixed with 100 μM [^{35}S]APS (10 Ci/mmol) (final concentrations). Reactions were stopped by mixing to a final concentration of 50 mM EDTA, 200 mM KOH, and 10 μM PAP in 10% glycerol. The reaction products were seperated on PEI TLC plates using 1 M LiCl as the solvent. The radioactivity associated with the spots on the TLC plate was quantified using a two-dimensional AMBIS radioactivity detector. The rate constants were obtained by fitting the data to a first-order rate equation using the program EnzFitter (Elsevier Biosoft).

RESULTS

Rapid Chemical Quench Kinetic Studies. To verify whether the phosphoenzyme formed in the APS kinase reaction was kinetically viable as an intermediate on the normal reaction pathway, we carried out rapid-quench experiments to determine the rate of phosphorylation of APS kinase by saturating concentrations of ATP. When ATP at a concentration of $\sim$100 times the K_m was mixed with APS kinase, E-P was formed with a rate constant of 46 s^{-1} ((Figure 1A). Since V_{max} under these conditions is $\sim$45 s^{-1}, phosphorylation of the protein is kinetically competent to be on the overall reaction pathway at all substrate concentrations. In other rapid-quench experiments when E-P was mixed with APS the rate constant for PAPS formation was 91 s^{-1}, (Figure 1B) well in excess of V_{max}. The results suggest that phosphorylation of the enzyme is the rate-limiting step in the overall reaction.

Sequence of cysC. Since the phosphorylated enzyme is a kinetically viable reaction intermediate, we sought to locate the site of phosphorylation. This laboratory previously reported the cloning of a 9.4-kb DNA fragment which contains the *cysDNC* operon from *E. coli* (Leyh et al., 1988). The first two genes of this operon, *cysDN*, encode the two subunits of ATP sulfurylase and the third gene is the structural gene for APS kinase. The location of *cysC* on the cloned DNA was deduced by deletions of the 9.4-kb chromosomal fragment (Leyh et al., 1988). To allow the identification of a proper reading frame for *cysC*, the amino terminal sequence of the purified protein was determined, yielding the sequence ALHDENVV. Previous insertion mutagenesis studies indicated that the promoter for the *cysDNC* operon precedes *cysD* and thus is approximately 2.5-kB upstream of *cysC*. Therefore, the identification of a promoter for *cysC* was not attempted, and only the coding region of *cysC* was sequenced. The complete DNA sequence of *cysC* and the deduced protein sequence are shown in Figure 2. The N-terminal methionine is not present in the purified enzyme. The open reading frame codes for protein of 22 321 Da, in good agreement with the value of 21 kDa estimated by SDS–polyacrylamide gel electrophoresis (Satishchandran & Markham, 1989). The native protein undergoes dimer–tetramer interconversions depending on experimental conditions and the phosphorylation state (Satishchandran & Markham, 1989).
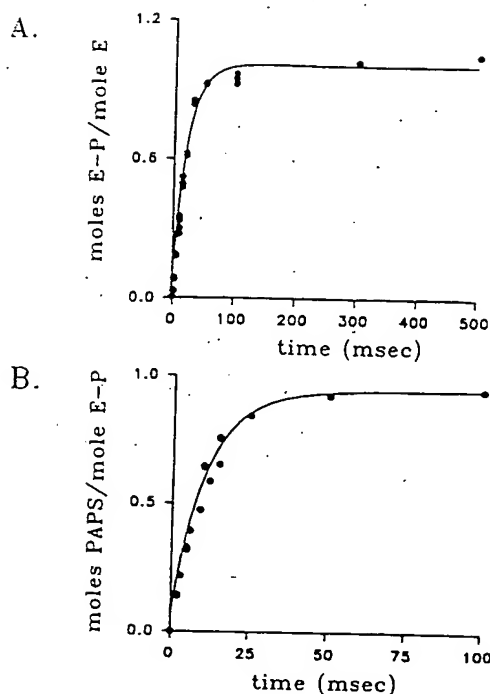
A.

B.

FIGURE 1: Rapid quench kinetics of phosphoryl group transfer. (A) Rate of phosphorylation of APS kinase by ATP. The solutions contained final concentrations 62.5 μM APS kinase and 0.5 mM [γ-^{32}P]ATP in 50 mM Hepes/KOH, 50 mM KCl, 1 mM MgCl$_2$, and 10% glycerol, pH 8.0. After incubation for the times shown, the reactions were quenched by mixing with 10% TCA (final concentration) in 10% glycerol. The ^{32}P present in the precipitated protein was quantified as described in Materials and Methods. (B) Rate of phosphorylation of APS by E-P. Solutions contained 100 μM [^{35}S]-APS, 12.5 μM APS kinase in 50 mM Hepes/KOH, 50 mM KCl, 1 mM MgCl$_2$, and 10% glycerol, pH 8.0. The reactions were quenched with 50 mM EDTA, 200 mM KOH, and 10 μM PAP (final concentrations) in 10% glycerol. The lines drawn are the best fits to a first-order rate equation, with rate constants of 46 (A) and 91 s^{-1} (B). The standard deviations in the rate constants are 4% (A) and 9% (B).

Examination of the codon utilization (Table I) indicates that the fourth and fifth codons, encoding histidine and aspartate, are among those least (<1%) used in *E. coli*, while most other codons are among the more commonly employed. The use of low-frequency codons at the beginning of the coding region and the absence of a consensus ribosome binding sequence (Shine & Dalgarno, 1974) within the 15 nucleotides preceding the start codon might account for the ~70-fold lower production of APS kinase compared to the *cys*DN gene products, even when RNA production is driven using a bacteriophage T7 promoter and T7 RNA polymerase. The presence of sequence motifs suggesting locations of substrate binding sites is discussed below.

Identification of the Phosphorylated Residue Type. We had previously reported that the phosphoryl linkage in E-P is quite stable, surviving gel filtration and SDS–gel electrophoresis. Before attempting to determine which residue was phosphorylated, we sought to elucidate the type of residue to which the phosphoryl group was attached, as this knowledge would aid in the choice of an appropriate protease and of chromatographic conditions for peptide isolation. The ^{31}P NMR spectrum of a 0.1 mM solution of the phosphorylated enzyme showed a single peak at 4.3 ppm, demonstrating that the phosphoryl group was present in a phosphomonoester linkage (Vogel, 1989); however, the line was too broad (~10 Hz) for ^{1}H coupling to be resolved in the absence of ^{1}H decoupling. The ^{31}P NMR spectrum of E-P denatured by incubation for several hours at 25 °C showed that the 4.3 ppm NMR resonance was replaced by a sharper new peak at 4.8

ppm, a chemical shift also characteristic of a phosphomonoester. In the absence of ^{1}H decoupling, the 4.8 ppm resonance was a triplet ($^3J_{P-H}$ = 6.5 Hz) indicating a CH$_2$-O-P linkage. The chemical shift of 4.3 ppm, the P-H coupling constant, and multiplicity coincide with those of a phosphoserine standard under these conditions. Thus the NMR data conclusively identify the phosphorylated residue as a serine, one of 11 serine residues in the sequence. Due to local environmental effects in the native protein, the ^{31}P resonance is shifted downfield by 0.5 pppm from free phosphoserine; unfortunately, the interpretation of small changes in ^{31}P chemical shifts is not yet unambiguous (Gorenstein, 1989).

Identification of the Phosphorylated Serine. To identify the serine which is phosphorylated, ^{32}P-labeled E-P was proteolytically cleaved with *Staphylococcal* V8 protease. Peptides were separated by reverse-phase HPLC. A single peak containing ^{32}P was obtained. The composition of the peptide was determined and is shown in Table II where it is compared to the predicted amino acid composition for the peptide encompassing residues 98–113. An excellent correlation is observed, while no other predicted peptides gave compositions that were remotely similar to the observed composition. Since there is only one serine in this peptide, the phosphorylation site is identified as serine-109.

Sequence Motifs in cysC. When the deduced protein sequence of APS kinase was compared with the collection of consensus sequences present in the ProSite database (Release 8.0), a perfect match with the purine nucleotide binding site consensus sequence G-x-x-x-x-G-K-S (Walker et al., 1982) was seen starting at residue 35, as GLSGSGKS (Figure 2, in box). The motif is also present in the APS kinase sequences from *S. cerevisiae* and *R. meliloti* (Korch et al., 1991; Schwedock & Long, 1990). The oncogene product H-rasp21 displays a motif similar to the purine nucleotide binding motif in APS kinase. The 1.35-Å X-ray crystal structure of H-rasp21 complexed with β-γ-imido-GTP reveals the primary interaction of the amino acids in the purine nucleotide binding motif to be with the β-phosphoryl group of the nucleotide (Pai et al., 1990). Our observation that the serine that is phosphorylated in the APS kinase reaction is not the serine present in this motif is consistent with the interactions predicted from the studies on rasp21.

We compared the deduced *E. coli* APS kinase sequence with those of *S. cerevisiae* and the C-terminal region of the *nod*Q protein [a subunit of a bifunctional ATP sulfurylase/APS kinase (Schwedock, 1991)]. The *E. coli* enzyme has 47.9% identity over a 200 amino acid region to the yeast enzyme and 54.9% identity over a 195 amino acid region to the C-terminal portion of the *R. meliloti* enzyme. The ATP consensus sequence and the sequence FISP containing serine-109 are identical in all three enzymes. The phosphorylation of the *S. cerevisiae* or the *R. meliloti* proteins has not been reported, nor have the mechanisms of these enzymes been extensively studied.

In an effort to discern a motif which might be related to PAPS binding, we compared the APS kinase sequences with sequences available for enzymes which are involved in PAPS utilization: bovine estrogen sulfotransferase (Nash et al., 1988), rat hydroxysteroid sulfotransferase (Ogura et al., 1989), rat alcohol sulfotransferase (Ogura et al., 1990), rat aryl sulfotransferase (Ozawa et al., 1990), *R. meliloti* nodulation factor sulfotransferase (Roche et al., 1991), two plant (*Flaveria chloraefolia*) flavol sulfotransferases (Varin et al., 1992), *E. coli* PAPS reductase (*cysH*) (Ostrowski et al., 1989), and a rat senescence-related protein with high sequence homology to the mammalian sulfotransferases (Chaterjee et al., 1987).

```
        -10              1
    CTG GGG GGA TAA ATA ATG GCG CTG CAT GAC GAA AAC GTC GTC TGG CAT AGC
                        Met Ala Leu His Asp Glu Asn Val Val Trp His Ser    12


    CAT CCG GTC ACT GTG CAA CAA CGC GAG CTA CAC CAC GGT CAT CGT GGT GTA
    His Pro Val Thr Val Gln Gln Arg Glu Leu His His Gly His Arg Gly Val    29

                    100            ATP MOTIF
    GTG CTG TGG TTT ACC GGC CTC TCC GGG TCC GGT AAA TCA ACG GTC GCC GGG
    Val Leu Trp Phe Thr GLY Leu Ser Gly Ser GLY LYS SER Thr Val Ala Gly   46


    GCG CTG GAG GAG GCG TTA CAT AAA CTC GGC GTC AGT ACG TAT CTG CTG GAT
    Ala Leu Glu Glu Ala Leu His Lys Leu Gly Val Ser Thr Tyr Leu Leu Asp   63

                    200
    GGC GAC AAT GTT CGC CAC GGA TTA TGC AGC GAT CTC GGT TTT AGC GAT GCC
    Gly Asp Asn Val Arg His Gly Leu Cys Ser Asp Leu Gly Phe Ser Asp Ala   80


    GAT CGT AAA GAG AAT ATC CGT CGC GTC GGT GAA GTG GCG AAT TTG ATG GTT
    Asp Arg Lys Glu Asn Ile Arg Arg Val Gly Glu Val Ala Asn Leu Met Val   97

            300                          P-Ser
    GAA GCC GGA CTG GTG GTG CTG ACC GCA TTT ATC TCG CCA CAC CGC GCC GAA
    Glu Ala Gly Leu Val Val Leu Thr Ala Phe Ile Ser Pro His Arg Ala Glu   114


    CGC CAG ATG GTT CGC GAA CGC GTA GGA GAA GGG CGC TTT ATC GAA GTG TTT
    Arg Gln Met Val Arg Glu Arg Val Gly Glu Gly Arg Phe Ile Glu Val Phe   131

            400
    GTC GAT ACG CCG CTG GCG ATT TGC GAA GCC CGC GAT CCC AAA GGC TTA TAT
    Val Asp Thr Pro Leu Ala Ile Cys Glu Ala Arg Asp Pro Lys Gly Leu Tyr   148

                    PAPS MOTIF
    AAG AAA GCG CGT GCC GGT GAA CTG CGC AAC TTT ACG GGA ATA GAT TCC GTT
    Lys LYS ALA Arg Ala GLY Glu Leu Arg ASN PHE THR Gly Ile Asp Ser Val   166
        500
    TAC GAA GCG CCT GAA TCG GCA GAA ATT CAT CTC AAT GGT GAA CAA TTA GTA
    Tyr Glu Ala Pro Glu Ser Ala Glu Ile His Leu Asn Gly Glu Gln Leu Val   183


    ACA AAT TTG GTA CAG CAA TTA TTA GAT CTG TTG AGA CAG AAC GAT ATT ATC
    Thr Asn Leu Val Gln Gln Leu Leu Asp Leu Leu Arg Gln Asn Asp Ile Ile   200

        600
    AGA TCC TGA
    Arg Ser End
```

FIGURE 2: Sequence of *cysC* and deduced amino acid sequence of APS kinase. The serine phosphorylated upon incubation with ATP is enclosed in double lines. A sequence consistent with an ATP binding motif and the region containing a sequence present in sequences of 10 reported PAPS-utilizing proteins are boxed. For both motifs, the residues agreeing with the consensus are capitalized in bold type. Numbers above the sequence refer to nucleotides, while numbers at the right refer to amino acids.

A common sequence, K(A/G)xxGxxx(N/E)x(0 or 1)FT, is present in all these sequences (Figure 3), with the exception of the PAPS reductase, which has no sequences resembling this motif. Comparison of groups consisting solely of either APS kinases or sulfotransferases was not useful in these analyses since within these groups the sequences are too similar to one another. This motif begins between 35 and 69 residues from the carboxy terminus of each protein. This motif did not appear either in the sequence of yeast ATP sulfurylase (Cherest et al., 1987) or in the *nodP* component of the bifunctional *R. meliloti* ATP sulfurylase/APS kinase (Schwedock & Long, 1990; Schwedock, 1991). In order to test whether this motif might be useful in identifying PAPS-utilizing proteins, the consensus was tested against the databases PIR-protein and Swissprot with all possible combinations of residues in the X positions; only the proteins used in constructing the sequence were found, suggesting that this may be a PAPS-related motif. Since no PAPS binding sites have yet been identified by affinity labeling, the functional significance of this motif is unclear.

Table I: Summary of Codon Usage for *cysC*[a]

Phe	TTT	6	Ser	TCT	0	Tyr	TAT	2	Cys	TGT	0
Phe	TTC	0	Ser	TCC	4	Tyr	TAC	1	Cys	TGC	2
Leu	TTA	6	Ser	TCA	1		TAA	0[b]		TGA	1[b]
Leu	TTG	3	Ser	TCG	2		TAG	0[b]	Trp	TGG	2
Leu	CTT	0	Pro	CCT	1	His	CAT	6	Arg	CGT	4
Leu	CTC	4	Pro	CCC	1	His	CAC	4	Arg	CGC	10
Leu	CTA	1	Pro	CCA	1	Gln	CAA	4	Arg	CGA	0
Leu	CTG	10	Pro	CCG	2	Gln	CAG	3	Arg	CGG	0
Ile	ATT	3	Thr	ACT	1	Asn	AAT	5	Ser	AGT	1
Ile	ATC	4	Thr	ACC	1	Asn	AAC	3	Ser	AGC	3
Ile	ATA	1	Thr	ACA	1	Lys	AAA	4	Arg	AGA	2
Met	ATG	3	Thr	ACG	4	Lys	AAG	1	Arg	AGG	0
Val	GTT	4	Ala	GCT	0	Asp	GAT	9	Gly	GGT	7
Val	GTC	7	Ala	GCC	6	Asp	GAC	2	Gly	GGC	4
Val	GTA	4	Ala	GCA	2	Glu	GAA	13	Gly	GGA	4
Val	GTG	6	Ala	GCG	7	Glu	GAG	4	Gly	GGG	3

[a] The high usage codons utilized in *E. coli* are shown in italic, while the low usage codons are underlined (Zhang et al., 1991). [b] Termination codons.

Table II: Predicted and Observed Amino Acid Compositions of the Phosphorylated Peptide[a]

	residues 98–113			residues 98–113	
	predicted	obsd		predicted	obsd
Ala	3	3.3	Ser + P-Ser	1	1.3
Gly	1	1.3	Pro	1	1.3
Leu	2	2.1	His	1	0.9
Val	2	1.7	Arg	1	1.0
Thr	1	1.2	Glu	1	0.8
Phe	1	0.8	all others	0	<0.2

[a] Predictions are based on the deduced amino acid sequence of the protein. No other peptides have similar compositions. Compositions are the average of three determinations and are normalized to arginine. P-Ser is unstable when subjected to acid hydrolysis, and the P-ser/serine ratio was variable in different determinations [P-ser/(P-ser + Ser) = 0.4–0.6]. Serine is the product of P-Ser hydrolysis, and therefore, P-Ser and Ser are presented together.

285	RKAKDGDWKNYFTD	FST-1
276	RKGKDGDWKNYFTD	FST-2
246	RKGTVGDWKNHFTV	AST
246	RKGTVGDWKNHFTV	HSST
244	RKGTTGDWKNHFTV	S-MP2
253	RKGTTGDWKNTFTV	ArST
257	RKGDVGDWKNHFTV	EST
149	KKAREGVIKE-FTG	*cysC*
147	EKALAGKIAN-FTG	*met14*
581	KKARAGELRN-FTG	*nodQ*

FIGURE 3: Alignment of sequences of PAPS-utilizing proteins in region of proposed PAPS binding site. The set of residues in the consensus is shown in white upon black. From top to bottom the sequences are as follows: flavol sulfotransferase-1, flavol sulfotransferase-2, alcohol sulfotransferase, hydroxysteroid sulfotransferase, senescence-related marker protein 2, aryl sulfotransferase, estrogen sulfotransferase, E. coli APS kinase, S. cerevisiae APS kinase, and R. meliloti nodQ protein (APS kinase domain).

DISCUSSION

These results demonstrate that both phosphorylation of APS kinase on serine-109 by ATP and transfer of the phosphoryl group of E-P to APS are rapid enough to represent steps in the mechanism, even at V_{max} conditions. APS kinase contains an ATP binding motif near the amino terminus and an apparent PAPS binding motif near the carboxy terminus. The serine that is phosphorylated is located between these motifs. Previous studies have indicated that, at very low (physiological) APS concentrations, the APS kinase reaction can occur by a ping-pong kinetic mechanism where no ternary E·ATP·APS complex forms, while at higher APS concentrations a E·ATP·APS complex occurs on the reaction pathway (Satishchandran & Markham, 1989). The phosphorylated enzyme can participate in either steady-state route. Although the steady-state kinetic behavior of the APS kinase from *P. chrysogenum* is quite similar to that of the *E. coli* enzyme, the fungal enzyme apparently does not form a stable phosphoenzyme (Renosto et al., 1991). However, the formation of an APS-dependent transient phosphorylated enzyme intermediate has not been excluded (Renosto et al., 1991). The sequence of the fungal enzyme has not been reported; thus the structural similarity of the two enzymes is as yet unclear. Whether the phosphorylated *E. coli* enzyme is involved in the overall reaction under all conditions remains to be determined by site-directed mutagenesis of serine-109 and from elucidation of the stereochemical course of phosphoryl transfer. If the phosphorylated protein is an obligatory intermediate in the APS kinase reaction, the distant sequence locations of the ATP and PAPS binding motifs might suggest that the two substrate binding sites are not close enough in space to allow direct phosphoryl transfer and suggest a role for the phosphoserine analogous to the biotin "swinging arm" mechanism (Northrup & Wood, 1969; Wood, 1972).

REFERENCES

Baddiley, J., Buchanan, J. G., & Letters, R. (1957) *J. Chem. Soc.* 1067–1071.

Chaterjee, B., Majurdar, D., Ozbilen, O., Murty, C. V. R., & Roy, A. K. (1987) *J. Biol. Chem. 262*, 822–825.

Cherest, H., Kerjan, P., & Surdin-Kerjan, Y. (1987) *Mol. Gen. Genet. 210*, 307–313.

Clark, S. (1992) (submitted for publication).

Devereux, J., Haeberli, P., & Smithies, O. (1984) *Nucleic Acids Res. 12*, 387–395.

Falany, C. N. (1991) *Trends Pharm. Sci. 12*, 255–260.

Garces, E., & Cleland, W. R. (1969) *Biochemistry 8*, 633–640.

Gorenstein, D. G. (1989) *Methods Enzymol. 177*, 295–316.

Huxtable, R. I. (1986) *The Biochemistry of Sulfur*, Plenum Press, New York.

Jaffe, E. K., Abrams, W. R., Kaempfen, K. X., & Harris, K. A. (1992) *Biochemistry 31*, 2113–2123.

Knowles, J. R. (1980) *Annu. Rev. Biochem. 49*, 877–819.

Korch, C., Mountain, H. A., & Byström, A. S. (1991) *Mol. Gen. Genet. 229*, 96–108.

Leyh, T. S., Taylor, J. T., & Markham, G. D. (1988) *J. Biol. Chem. 263*, 2409–2916.

Nash, A. R., Glenn, W. K., Moore, S. S., Kerr, J., Thompson, A. R., & Thompson, E. O. (1988) *Aust. J. Biol. Sci. 41*, 507–516.

Northrup, D. B., & Wood, H. G. (1969) *J. Biol. Chem. 244*, 5820–5827.

Ogura, K., Kajita, J., Narihata, H., Watabe, T., Ozawa, S., Nagata, K., Yamazoe, Y., & Kato, R. (1989) *Biochem. Biophys. Res. Commun. 165*, 168–174.

Ogura, K., Kajita, J., Narihata, H., Watabe, T., Ozawa, S., Nagata, K., Yamazoe, Y., & Kato, R. (1990) *Biochem. Biophys. Res. Commun. 166*, 1494–1500.

Ostrowski, J., Wu, J.-Y., Rueger, D. C., Miller, B. E., Siegel, L. M., & Kredich, N. M. (1989) *J. Bacteriol. 171*, 130–140.

Ozawa, S., Nagata, K., Gong, D., Yamazoe, Y., & Kato, R. (1990) *Nucleic Acids Res. 18*, 4001.

Pai, E. F., Krengel, U., Petsko, G. A., Goody, R. S., Kabsch, W., & Wittinghofer, A. (1990) *EMBO J. 9*, 2351–2359.

Pearson, W. R. (1990) *Methods Enzymol. 183*, 63–98.

Renosto, F., Martin, R. L., & Segel, I. H. (1991) *Arch. Biochem. Biophys. 284*, 30–34.

Satishchandran, C., & Markham, G. D. (1989) *J. Biol. Chem. 264*, 15012–15021.

Schwedock, J. (1991) Ph.D. Thesis, Stanford University.

Schwedock, J. & Long, S. R. (1990) *Nature 348*, 644–647.

Shine, J., & Dalgarno, L. (1974) *Proc. Natl. Acad. Sci. U.S.A. 68*, 367–371.

Varin, L., DeLuca, V., Ibrahim, R. K., & Brisson, N. (1992) *Proc. Natl. Acad. Sci. U.S.A. 89*, 1286–1290.

Vogel, H. J. (1989) *Methods Enzymol. 177*, 263–282.

Walker, J. E., Saraste, M., Runswick, M. J., & Gay, N. J. (1982) *EMBO J. 1*, 945–951.

Wood, H. G. (1972) in *The Enzymes* (Boyer, P. D., Ed.) Vol. 6, pp 83–116, Academic Press, New York.

Yount, R. G., Simchuck, S., Yu, I., & Kottke, M. (1966) *Arch. Biochem. Biophys. 113*, 288–295.

Zhang, S., Zubay, G., & Goldman, E. (1991) *Gene 105*, 61–72.

Short Sequence-Paper

A cDNA for adenylyl sulphate (APS)-kinase from *Arabidopsis thaliana*

Hildegard E. Arz, Günter Gisselmann, Sandra Schiffmann, Jens D. Schwenn *

Biochemistry of Plants, Faculty of Biology, Ruhr-University-Bochum, 44780 Bochum, Germany

Received 25 November 1993

Abstract

A cDNA clone with an open reading frame of 831 nucleotides was isolated from a λZapII-library of *Arabidopsis thaliana*. The nucleotide sequence of the cDNA is homologous to the APS-kinase genes from enterobacteria, diazotrophic bacteria, and yeast: *Escherichia coli* (*cys* C: 53.2%), *Rhizobium meliloti* (*nod* Q: 52.6%), and *Saccharomyces cerevisiae* (*met* 14: 57.1%). The polypeptide deduced from the plant APS-kinase cDNA is comprised of 276 amino acid residues with a molecular weight of 29790. It contains an N-terminal extension of 77 amino acids. This extension includes a putative transit peptide of 37 residues separated from the core protein by a VRACV processing site for stromal peptidase; a molecular weight of 26050 is predicted for the processed protein. The relatedness between bacterial, fungal and plant APS-kinase polypeptides ranges from 47.5% (*E. coli*), 55.4% (*S. cerevisiae*), 52.6% (*R. meliloti*), and 50.3% (*Azospirillum brasilense*). The plant polypeptide contains eight cysteine residues; two cysteines flank a conserved purine nucleotide binding domain: GxxxGK. Also conserved are a serine-182 as a possible phosphate transferring group and a K/LARAGxxxFTG motif described for PAPS dependent enzymes. The identity of the gene was confirmed by analyzing the function of the gene product. The putative transit peptide was deleted by PCR and the truncated gene was expressed in a pTac1 vector system. A polypeptide of MW 25761 could be induced by IPTG. The gene product was enzymatically active as APS-kinase. It produced PAPS from APS and ATP – the absence of ATP but supplemented with thiols, the APS-kinase reacted as APS-sulphotransferase. APS-sulphotransferase is not a separate enzyme but identical with APS-kinase.

Key words: APS-kinase; APS-sulphotransferase; cDNA sequence; Gene function; Plastidic protein; Protein expression; (*Arabidopsis thaliana*)

Sulphate is the oxidized form of sulphur which a plant can assimilate for the biosynthesis of its S-containing compounds. Sulphate is not reduced directly but adenylated by the enzymes ATP-sulphurylase (EC.2.7.7.4) and APS-kinase (2.7.1.25). The presence of ATP-sulphurylase and APS-kinase in higher plants has amply been demonstrated and both enzymes appear to be located in the plastid [37], yet the occurrence of isoenzymes in the cytosol has also to be taken into account [22]. The plant APS-kinase is difficult to

study [6,43] because of low specific concentration and obscuring side reactions degrading substrate or product. Today, most of the biochemical data are derived from work with non-phototrophic organisms like yeast or *Penicillium chrysogenum* [20,21,34] except for the enzyme from the green alga *Chlamydomonas reinhardii* which has been investigated in more detail [13,26].

It has been open to question whether plants and phototrophic bacteria require APS or PAPS as metabolite in the pathway of sulphate reduction like most enterobacteria and fungi. In these organisms, APS-kinase is required to synthesize PAPS which is reduced to sulphite by a thioredoxin dependent PAPS-reductase [25,40]. Higher plants, green algae and some phototrophic bacteria were proposed to reduce APS instead of PAPS through transfer of the sulphate group onto an unidentified thiol forming a bound sulphite. The activity responsible for this reaction was described as APS-sulphotransferase [1,30]. In comparison to the

free sulphite which in plants is metabolized by a ferredoxin dependent sulphite-reductase, Schmidt proposed that bound sulphite is reduced by a ferredoxin dependent thiosulphonate reductase [31]. This view was extended by an identification of glutathione as the carrier-thiol [45] and by the isolation of a homogeneous APS-sulphotransferase from Euglena [18]. The current view of this APS-bound sulphite pathway was compiled most recently [33]. Arguments that were raised against such a pathway focus primarily on the properties and reaction conditions of the APS-sulphotransferase and thiosulphonate reductase. As the plant APS-kinase has a high affinity for APS (< 2 μM) and ATP (8 μM [13]), the sulphotransferase would run out of substrate, even if PAPS is hydrolysed to APS by a specific phosphohydrolase as suggested by Tsang and Schiff [44]. Claims for a thiosulphonate reductase reducing exclusively bound sulphite to bound sulphide were questioned by Siegel [42] because of the inadequacy of the assay system. In addition, PAPS-reductase that was found in higher plants [41] formed free sulphite like the enzyme from enterobacteria or yeast. Formation of bound sulphite was shown to be due to artificial side reactions of free sulphite with disulphides [40].

In the past, biochemical and physiological methods proved insufficient to solve the question how sulphite is formed in plants. More recently, new data were obtained from investigations of the molecular biology of sulphate metabolism. It was found that the structural genes from cyanobacteria and plants encoding ATP-sulphurylase [14], PAPS-reductase [19], ferredoxin-sulphite reductase [10], and O-acetylserine (thiol) lyases [23,24,26] are homologous to their counterparts from enterobacteria and fungi. Also, no inconsistency in catalytic properties was found between recombinant gene products and enzyme proteins characterized previously. Thus, it seems feasible that the enzymatic steps of sulphate assimilation in photo-autotrophs are identical with reactions known from enterobacteria and yeast -- only that photo-autotrophic organisms can replace NADPH by ferredoxin. As a gene-enzyme correlation for this pathway in photo-autotrophic organisms would provide the necessary data, we started to isolate the corresponding genes from cyanobacteria and plants. This paper describes the primary structure of the APS-kinase gene and some properties of the gene product expressed from the Arabidopsis thaliana cDNA clone.

Media, strains and plasmids. Escherichia coli TG1, XL1-Blue (Genofit), and JM81A (B. Bachmann, ECG Yale) were grown in rich medium (LB) or for phenotypic complementation on Vogel-Bonner minial medium. When required for the plasmids (pBluescript II KS + and SK + from Genofit, pBTac1 from Boehringer) ampicillin was used at a concentration of 100 mg/l. Other methods for selection and induction were as described in Sambrook et al. [27]. Competent E. coli were prepared from freshly inoculated cultures following the Hanahan protocol 3 and transformed as described in Ref. 11; frozen competent cells were transformed accordingly.

DNA procedures. The plant type APS-kinase gene was derived from a cDNA of Arabidopsis thaliana L. Heynh. This cDNA library was kindly donated by D. Bartling, University Bochum [2]; it was cloned in a λZapII vector and amplified once. Clones with APS-kinase DNA were identified using an oligonucleotide which was deduced from highly conserved parts of the polypeptide sequences of Escherichia coli [29], and Saccharomyces cerevisiae [7,15]. With a DIG-labelled synthetic oligonucleotide cys C1 5'-TAT(C)A(T,C)T(G)IC(T)TIGAT(C)GGIGAT(C)AA-3' three positive plaques were detected. Only the clone in pATGG1/1 was characterized. The DNA was sequenced by the chain termination method using T3 and T7 universal primers. Overlapping clones were constructed from restriction fragments obtained with EcoRI, EcoRV, HindIII BamHI and StyI.

For construction of the truncated gene in pAKSS1 we used a PCR method[12] with two primers:

5'-primer: 5'-ATGGATGGATCTCAAACTCTG-3'
3'-primer: 5'-GTATCTA'GATCTATGTTATGCTT-GAAG-3'

The 5'-end of the gene was deleted to make the first ATG downstream of this putative processing site the start codon. At the 3'-end of the gene a BglII site 4 bp downstream of the stop codon was introduced using a mutated PCR-primer. After restriction, the PCR product is 718 bp in length including 7 bp downstream of the TAA codon. This treatment of the PCR-product produced a sticky 3'-end that is compatible with the BamHI site of the expression vector pBTac1. The ATG located at the 5'-blunt end of the gene was ligated into the EcoRI site of the vector, Klenow fragment was used to fill in the 3'-overhang. The construct, designated as pAKSS1, was verified by sequencing into the cloned gene from both directions with the help of universal pBTac1 primers.

Enzymatic methods. APS-kinase activity was measured as ATP-dependent formation of [35S]PAPS from [35S]APS. The nucleotides were separated by reversed-phase HPLC and quantitated as outlined previously [26]. [35S]APS was obtained by S1 nuclease treatment of [35S]PAPS which was synthesized with purified ATP-sulfurylase and APS-kinase from yeast as described previously [34]. APS-sulphotransferase activity was measured as described by Schmidt [32] and Brunold [5]. The specific radioactivity of substrate [35S]APS was diluted with unlabelled APS prepared enzymatically; all sulphonucleotides used as substrates were purified by ionexchange chromatography on DEAE-TSK.

For extraction of recombinant enzyme protein from transgenic host, bacteria were collected by centrifugation washed once in Tris-HCl 25 mM (pH 8.0) including EDTA 0.1 mM. The cells were disrupted by sonication (4 × 15 s), APS-kinase was extracted in Tris-HCl 100 mM (pH 8.0), EDTA 1 mM, $MgCl_2$ 10 mM, lysozyme 0.2 mg/ml, Triton X-100 0.1%. The buffer system for APS-sulphotransferase extraction contained Tris-HCl 100 mM (pH 8.0), KCl 100 mM, $MgCl_2$ 20 mM and β-mercaptoethanol 10 mM.

Gel electrophoresis, protein determination. Protein was determined according to Bradford [4]. SDS-PAGE was carried out as described by Laemmli [17] replacing mercaptoethanol in the sample buffer by dithiothreitol as indicated in the legend to Fig. 3. Other methods used for the determination of nucleic acids or nucleotides were as described in the corresponding chapters of the laboratory manuals [27].

A cDNA library from *Arabidopsis thaliana* (L.) var. Landsberg erecta was screened with a 128 × degenerated oligonucleotide. The nucleotide sequence of this probe was deduced from the YR/LDGDN amino acid sequence conserved in the *Escherichia coli* K12 [29], *Saccharomyces cerevisiae* [7,15] and *Rhizobium meliloti* [39] APS-kinase polypeptides. The cDNA from clone pATG1/1 was chosen for further sequencing. The whole DNA fragment in this plasmid was comprised of 1185 nt (Fig. 1). Assuming that the open reading frame started at position 42 with the first ATG codon, the putative gene contained 828 nt. The TAA-codon (position 872) was followed by a non-coding region that contained a polyadenylation sequence (5'-AATAAA-3') from nt 985 to 990. It is located in a palindromic sequence (nt 974–1021) which can form a hairpin structure; this structure is followed by a second palindromic sequence from nt 1083 to 1130. The 3'-adaptor sequence starts at position 1149 downstream of the poly(A) tail, yet, the 5'-adaptor was not located in the DNA sequenced. Sequence homology with the DNAs from bacterial or yeast APS-kinase genes is found from nt 269 to nt 872 (*E. coli* 53.2%, *cys* C and *Saccharomyces cerevisiae* 57%, *met* 14).

The amino acid sequence deduced from the cDNA is also highly similar (*cys* C 47.5%, *met* 14 55.6, and *nod* Q 52.6% in *R. meliloti*, 50.3% in *A. brasilense*). The predicted plant gene product is larger than the corresponding bacterial or fungal proteins: 29 790 Da in comparison to 22 231 (*E. coli* [30]) and 23 060 (*S. cerevisiae* [15]). Even though, it contains several clusters of conserved residues. This homology starts at asparagine-79 and continues over the entire length of the gene product including the C-terminal leucine-268 (Fig. 2). The T_{107}GLSGSGKST$_{116}$ sequence and the K_{222}LARAGxI/LxxFTGI$_{236}$ sequence have already been discussed by Markham for the polypeptide from *E. coli*. The motif GxxxGK---DxxG is assumed to

Fig. 1. Nucleotide sequence and deduced amino acid sequence of the cDNA identified as APS-kinase gene. DNA sequence of the cDNA clone pATG1/1 from an *Arabidopsis thaliana* λZapII library [2] with nucleotide residues (1–1185) numbered in 5'-3' direction. A polyadenylation sequence AATAA and the adaptor sequence CTC-GAGAC with the oligo(dT) sequence at the 3'-end are italicized, the 5'-adaptor is not recognizable in the sequence. The most probable eukaryotic translation start sequence is underlined, and both met residues of a putative transit peptide are indicated by arrows (Met-14 and Met-26), the position of the oligomer used for screening is also underlined; bold letters indicate the ATG used for construction of a truncated gene as required for expression of an enzymatically active APS-kinase in pBTac1.

belong to the ATP-binding niche [47] and the KA/GxAGxxxFTG motif was proposed to represent a group of PAPS metabolizing enzymes [29]. The PAPS motif may be true for the sulphate conjugating enzymes (transferases) only, because the proposal of a sulphonucleotide site does not apply to PAPS-reductases [3,19]. Serine-109 of the enzyme from *E. coli* was reported to become phosphorylated during catalysis [28,29]; this serine is conserved in the plant polypeptide. Its function as proposed appears unclear because the diazotrophic *Azospirillum brasilense* APS-kinase contains an alanine at the corresponding position. Yet, the residues flanking the alanine are conserved (i.e., FIAP instead of FISP), hence the possibility of a frame shift error can be excluded. If a serine becomes phosphorylated during catalysis it may be worthwhile to investigate one of the serines conserved in the ATP binding domain.

1. cysC   -   Escherichia coli
2. MET14   -   Saccharomyces cerevisiae
3. nod Q   -   Rhizobium meliloti
4.   -   Azospirillum brasilense
5. akn   -   Arabidopsis thaliana

Fig. 2. Comparison of the APS-kinase polypeptide sequences. The multiple alignment of APS-kinases from bacteria, yeast and a higher plant shows four highly conserved clusters of amino acids: the TGLSGSGKST sequence forms a nucleotide binding domain together with the RDPKGLY sequence which matches the GxxxGK-DxxG consensus sequence for GTP/ATP binding domains described by Dever et al. [8]. No function is assigned to the highly conserved regions DGDN and ENIRRVGEVA. The degenerated oligonucleotide primers used for gene amplification of homologous plant gene(s) were deduced from the LLDGDN- and RDPKGLY-sequence. Arrow indicates the putative processing site of the transit peptide by a stromal plastidic proteinase. Residue E_{16} was erroneously deleted from the MET14 sequence.

The high content of cysteine (8 per subunit) distinguishes the plant polypeptide from the bacterial proteins. Two of the cysteine residues flank the ATP-binding domain – the position of these two residues is identical with the cysteines of the yeast sequence – and another 'cysteine pair' flanks the serine in the F/LISP sequence. The four remaining cysteines appear randomly distributed with no homology in their position. It is not yet known which of these cysteines contribute to the stability of the enzyme or play a role during catalysis. Yet, from our previous investigation of the plant enzyme we know that the enzyme from *Chlamydomonas* is seriously affected by a thiol-disulphide redox charge [13,39]. It is rapidly inactivated by mercurials or alkylating inhibitors, by disulphides or oxidants. This oxidative type of inhibition was reversed by reducing thiols. Thioredoxin, at physiologically relevant concentrations, was found to stimulate the enzyme from *C. reinhardii* [32,39] by neutralizing the inhibitory effect

of high concentrations of substrates. In order to assign a function to any of the thiol groups site specific mutagenesis will be necessary.

The N-terminus forms a non-homologous extension consisting of 77 amino acids which are regarded as a part of a transit peptide. It is not yet clear which of the ATG codons serves as the translational start codon. A reasonable agreement with the plant consensus sequence A/T C/A AACAATGGCT is found at Met-26 with 8 identical bases out of 12 (AA--CAATG--T) – 7 identical bases were found when Met-14 is used as translational start codon (----C-ATGGCT). Of the imported polypeptides compared by Heijne [9] the majority starts with MAS. At present, it remains to be shown by analysis of amino acid sequence of the gene product which is the correct translational start. The molecular weight of the two resultant polypeptides would be with the Met-26: 27336 Da and with Met-14: 28572 Da. Whichever is the correct size of the transit peptide, it is separated by a > VRACVS < sequence from the core protein. This segment matches the motif of a processing site for stromal proteinases [9] which would process between alanine and cysteine. If indeed processed at this site and no further modification occurs after passage through the envelope inside of the chloroplast, a maximal mass of 26040 may be expected for the plastidic protein. From the only plant APS-kinase that was purified previously a molecular mass of 44 kDa was reported [13] for the denatured protein and 120 kDa for the native protein [13,37]. Since we now know that SDS-PAGE of the plant APS-kinase requires DTT instead of β-mercaptoethanol in order to obtain the monomeric form, we assume that the 44 kDa represented the dimer so that the native enzyme may be a homo-tetramer.

In general, APS-kinases are relatively small proteins with subunits ranging from 21 to 30 kDa and catalytically active proteins from yeast or *Penicillium* appear to be dimeric. For the plant enzyme a second processing step may be involved in order to reach a final mass of 22–23 kDa per subunit. Such a second digestion within the chloroplast [46] could be expected at residues 68 to 72 in a QKQGPL sequence. This second step would eliminate 32 amino acids reducing the size of a fully maturated APS-kinase down to 23 kDa.

In order to prove the identity of this gene by a analysis of the enzymatic property, a gene structure was needed which could be expressed in a suitable expression system. When compared with the known sequences from *E. coli* or yeast, the N-terminal extension seems dispensable for catalysis. We, therefore, deleted by PCR 161 bp of the 5'-non-homologous sequence. The truncated DNA starts with Met-41 and encodes for a polypeptide of 25761 Da. After induction by IPTG of the tac promoter, the formation of a new protein band with a molecular mass of 26 kDa was

observed only in hosts that harboured pAKSS1 (Fig. 3). In addition to this small peptide, a larger form with a mass of 52–54 kDa was observed – presumably representing the dimeric form of APS-kinase.

The identity of the cloned DNA as APS-kinase gene is shown in two ways: by complementation of a cys C-phenotype (E. coli JM81A) and by in vitro assay of the enzyme from cell homogenates after induction by IPTG (Table 1). Phenotypic complementation of JM81A was induced in 1080 transformants (90 transformants mg^{-1} DNA); this inefficient rate of transformation is assumed to be due to the wild type (rk$^+$ rm$^+$) host restriction system of JM81A. Yet, 8 transformants were isolated which grew well on minimal medium without induction. The corresponding colonies from these isolates were considerably larger on rich medium than those from IPTG inducible transformants or from wild type E. coli K12 (data not shown).

The activity of APS-kinase was already detectable from crude cell homogenates. Rates extrapolated from duplicates were 26 to 39 nmol PAPS mg^{-1} protein min^{-1} (Table 1). Endogeneous APS-kinase of the bacterial host was below detection; it is effectively repressed in enterobacteria grown on rich medium [16]. The activity in the pAKSS1 transformants, however, appears very high for a heterologous system. The rate obtained with the recombinant Arabidopsis enzyme

Table 1
Expression of the plant APS-kinase gene

Source of cell extract	Activity (nmol mg^{-1} min^{-1})	
	APS-kinase	APS-sulphotransferase
E. coli TG1	not detectable	0
+ vector (pBTac 1)	not detectable	0
+ pAKSS1	26–39	0.015

Measurement of APS-kinase in imidazol-HCl 25 mM (pH 6.8). MgCl$_2$ 2 mM, dithiothreitol 5 mM, APS 20 mM (specific activity: 535 Bq/nmol [^{35}S]APS), ATP 200 mM Na$_2$SO$_3$ 8 mM, cell extract 15 mg protein in a reaction volumn of 100 μl incubation 30 min at 25°C reaction started by addition of substrates APS and ATP, detection of PAPS by radio-HPLC [25]. APS-sulphotransferase is assayed in Tris-HCl 42 mM (pH 9.0), MgCl2 8 mM, DTT 8 mM, Na$_2$SO$_4$ 0.33 M, APS 45 μM (specific activity: 210 Bq/nmol), 1 mg protein (concentrated by precipitation with ammonium sulphate) in a reaction volumn of 600 ml; incubation 60 min, 37°C, terminated by addition of 100 mmol Na$_2$SO$_3$ and 300 ml of 3 M H$_2$SO$_4$, acid volatile SO$_2$ is trapped in 1 ml trioctylamine.

compares well with the extracts from Chlamydomonas reinhardii; APS-kinase from this alga formed PAPS at a rate ranging from 2 to 6 nmol PAPS mg^{-1} min^{-1} [13,26]. Extracts from wild type E. coli (AN1460) required concentration before 0.16 nmol PAPS mg^{-1} min^{-1} could be obtained [34]. Similarly, Renosto et al. reported that the APS-kinase from Penicillium chrysogenum was not measurable in crude extracts unless purified by affinity chromatography [20,21] – yeast seemed to contain a more active APS-kinase (0.6 to 13.6 nmol PAPS mg^{-1} min^{-1}) [34], yet considerably higher rates (18 nmol PAPS mg^{-1} min^{-1}) were only reported for a recombinant enzyme from an overproducing strain of E. coli [28] harbouring the structural gene cys C on a pT7-5 plasmid.

APS-kinase exhibits a side activity which is identical with the APS-sulphotransferase. Provided with APS and a reducing thiol, the enzyme from Arabidopsis thaliana formed sulphite (Table 1) in an assay as outlined in Refs. 5,32. It required high concentrations of protein in a high alkaline buffer system (pH > 9), supplemented with sulphate and dithiothreitol. Under these conditions, the activity of sulphite formation (15 pmol SO$_3^{2-}$ mg^{-1} min^{-1}) must be regarded as a side reaction of the APS-kinase under non-physiological conditions. Sulphite formation by plant APS-kinase was already described earlier [37,38] and it should be noted here that APS-kinase also responds to high ionic strength [20,22]. Hence, the high concentration of salts that was suggested to stimulate the transferase reaction (0.6 M Na$_2$SO$_4$ sulphate in Ref. 5, 0.8 M MgSO$_4$ and 0.2 M Na$_2$SO$_3$ in Ref. 32) may have supported the binding of APS as suggested in Ref. 28. The high-salt effects may be important in vitro – only a regulation by thioredoxin of the APS-kinase [34,39] may be physiologically relevant.
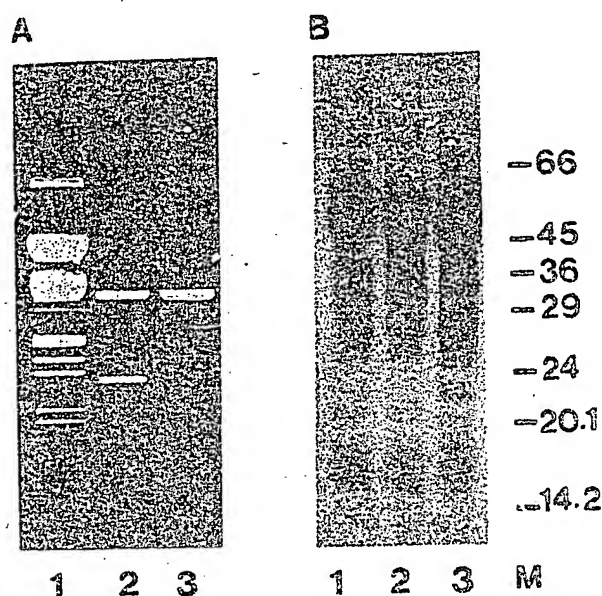

Fig. 3. Expression of pAKSS1 in Escherichia coli. (A) Restriction of pAKSS1 with Sal1 propagated in E. coli TG1; lane 1, lambda EcoRI/HindIII fragments: 2, pAKSS1 digested with Sal1, the insert size is 1.2 kb; lane 3, AKSS1. (B) SDS polyacrylamide gel electrophoresis of cell extracts (12.5 mg protein): lane 1, E. coli TG 1 as host; lane 2, transformants with pBTac1; lane 3, transformants as before harbouring pAKSS1, induced by IPTG. DTT (10 mM) was used in the sample buffer instead of mercaptoethanol; M, marker size is 14.2, 20.1, 24, 29, 36, 45, and 66 kDa.

References

[1] Abrams, W.A. and Schiff, J.A (1973) Arch. Mikrobiol. 94, 1–10.
[2] Bartling, D., Radzio, R., Steiner, U. and Weiler, E.W. (1993) Eur. J. Biochem. 216, 579–586.
[3] Berendt, U., Haverkamp, T. and Schwenn, J.D. (1993) unpublished data.
[4] Bradford, M.M. (1976) Anal. Biochem. 72, 248–254.
[5] Brunold, C. and Suter, M. (1990) in Methods in Plant Biochemistry, Vol. III (Lea, P.J., ed.), pp. 339–343.
[6] Burnell, J.N. and Anderson, J.W. (1973) Biochem. J. 134, 565–579.
[7] Cherest, H., Kerjan, P. and Surdin-Kerjan, Y. (1987) Mol. Gen. Genet. 210, 307–313.
[8] Dever, T.E., Glynias, M.J. and Merric, W.C.(1987) Proc. Natl. Acad. Sci. USA 84, 1814–1818.
[9] Gavel, Y. and Von Heijne, G. (1990) FEBS Lett. 261, 455–458.
[10] Gisselmann, G., Klausmeier, P. and Schwenn, J.D. (1993) Biochim. Biophys. Acta 1144, 102–106.
[11] Hanahan, D. (1985) in DNA Cloning, Vol. I (Glover, D.M., ed.), pp. 109–136, IRL Press, Oxford.
[12] Horton, R.McA. and Pease, L.R. (1991) in Directed Mutagenesis (McPherson, M.J., ed.), pp. 217–247, IRL Press, Oxford.
[13] Jender, H.G. and Schwenn, J.D. (1984) Arch. Microbiol. 138, 9–14.
[14] Klonus, D., Höfgen, R., Willmitzer, L. and Riesmeier, J.W. (1993) unpublished data.
[15] Korch, C., Mountain, H.A. and Byström, A.S. (1991) Mol. Gen. Genet. 229, 96–108.
[16] Kredich, N.M. (1987) in Amino Acids: Biosynthesis and Genetic Regulation (Herrmann, K.H. and Somerville, R.L., eds.), pp. 115–135, Addison Wesley, London.
[17] Laemmli, U.K. (1970) Nature 227, 680–685.
[18] Li, J. and Schiff, J.A. (1991) Biochem. J. 274, 355–360.
[19] Niehaus, A., Gisselmann, A. and Schwenn, J.D. (1992) Plant Mol. Biol. 20, 1179–1183.
[20] Renosto, F., Seubert, A. and Segel, I.H. (1984) J. Biol. Chem. 259, 2113–2123.
[21] Renosto, F., Martin, R.L. and Segel, I.H. (1991) Arch. Biochem. Biophys. 284, 30–34.
[22] Renosto, F., Patel, H.C., Martin, R.L., Thomassian, C., Zimmerman, G. and Segel, I.H. (1993) Arch. Biochem. Biophys. 307, 272–285.
[23] Römer, S., D'Harlingue, A., Camara, B., Schantz, R. and Kuntz, M. (1992) J. Biol. Chem. 267, 17966–17970.
[24] Rolland, N., Droux, M., Lebrun, M. and Douce, R. (1993) Arch. Biochem. 300, 213–222.
[25] Russel, M., Model, P. and Holmgren, A. (1989) J. Bacteriol. 172, 1923–1929.
[26] Saito, K., Miura, N., Yamazaki, M., Hirano, H. and Murakoshi, I. (1992) Proc. Natl. Acad. Sci. USA 89, 8078–8082.
[27] Sambrook, J., Fritsch, E.F. and Maniatis, T. (1989) Molecular Cloning, a Laboratory Manual, CHS Press, Cold Spring Harbor.
[28] Satishchandran, C. and Markham, G.D. (1989) J. Biol. Chem. 264, 15012–15021.
[29] Satishchandran, C., Hickman, Y.N. and Markham, G.D. (1992) Biochemistry 31, 11684–11688.
[30] Schmidt, A. (1972) Arch. Mikrobiol. 84, 77–86.
[31] Schmidt, A. (1973) Arch. Mikrobiol. 93, 29–52.
[32] Schmidt, A. (1976) Planta 130, 257–263.
[33] Schmidt, A. and Jäger, K. (1992) Annu. Rev. Plant Physiol. Plant. Mol. Biol. 43, 325–349.
[34] Schriek, U. and Schwenn, J.D. (1986) Arch. Microbiol. 145, 32–38.
[35] Schwedock, J. and Long, S.R. (1989) Mol. Plant Microb. Interact. 2, 181–194.
[36] Schwenn, J.D. and Jender, H.G. (1980) J. Chromatogr. 193, 285–290.
[37] Schwenn, J.D. and Urlaub, H.(1981) in Biology of Inorganic Nitrogen and Sulfur (Bothe, H.H and Trebst, A., eds), pp. 334–340, Springer, Berlin.
[38] Schwenn, J.D. and Jender, H.G. (1981) Phytochemistry 20, 601–604.
[39] Schwenn, J.D. and Schriek, U. (1984) FEBS Lett. 170, 76–80.
[40] Schwenn, J.D., Krone, F.A. and Husmann, K. (1988) Arch. Microbiol. 150, 331–319.
[41] Schwenn, J.D. (1989) Z. Naturforschg. 44c, 504–508.
[42] Siegel, L.M. (1976) in Metabolism of Sulfur Compounds, Vol. VII (Greenberg, D.M., ed.), p. 227, Academic Press, New York.
[43] Stanley, P.E., Kelley, B.C., Tuovinen, O.H. and Nicholas, D.J.D (1975) Anal. Biochem. 67, 540–551.
[44] Tsang, M.L.-S. and Schiff, J.A. (1976) Eur. J. Biochem. 65, 113–121.
[45] Tsang, M.L.-S. and Schiff, J.A. (1978) Plant Sci. Lett. 11, 177–183.
[46] vonHeijne, G., Steppuhn, J. and Herrmann, R.G. (1989) Eur. J. Biochem. 180, 535–545.
[47] Walker, J.E., Saraste, M., Runswick, M.J. and Gay, N.J. (1982) EMBO J. 1, 945–951.

# Crystal Structure of Adenosine 5′-Phosphosulfate Kinase from *Penicillium chrysogenum*[†,‡]

Ian J. MacRae,[§] Irwin H. Segel,[§] and Andrew J. Fisher*[,§,‖]

Department of Chemistry and Section of Molecular and Cellular Biology, University of California, One Shields Avenue, Davis, California 95616

Received October 18, 1999

ABSTRACT: Adenosine 5′-phosphosulfate (APS) kinase catalyzes the second reaction in the two-step conversion of inorganic sulfate to 3′-phosphoadenosine 5′-phosphosulfate (PAPS). This report presents the 2.0 Å resolution crystal structure of ligand-free APS kinase from the filamentous fungus, *Penicillium chrysogenum*. The enzyme crystallized as a homodimer with each subunit folded into a classic kinase motif consisting of a twisted, parallel β-sheet sandwiched between two α-helical bundles. The Walker A motif, [32]GLSASGKS[39], formed the predicted P-loop structure. Superposition of the APS kinase active site region onto several other P-loop-containing proteins revealed that the conserved aspartate residue that usually interacts with the Mg^{2+} coordination sphere of MgATP is absent in APS kinase. However, upon MgATP binding, a different aspartate, Asp 61, could shift and bind to the Mg^{2+}. The sequence [156]KAREGVIKEFT[166], which has been suggested to be a (P)APS motif, is located in a highly protease-susceptible loop that is disordered in both subunits of the free enzyme. MgATP or MgADP protects against proteolysis; APS alone has no effect but augments the protection provided by MgADP. The results suggest that the loop lacks a fixed structure until MgATP or MgADP is bound. The subsequent conformational change together with the potential change promoted by the interaction of MgATP with Asp 61 may define the APS binding site. This model is consistent with the obligatory ordered substrate binding sequence (MgATP or MgADP before APS) as established from steady state kinetics and equilibrium binding studies.

The activation of inorganic sulfate to 3′-phosphoadenosine 5′-phosphosulfate (PAPS)[1] proceeds in two steps that are catalyzed, in order, by ATP sulfurylase (MgATP:sulfate adenylyltransferase, EC 2.7.7.4) and APS kinase (MgATP: APS 3′-phosphotransferase, EC 2.7.1.25):

$$MgATP + SO_4^{2-} \square \ MgPP_i + APS \ (ATP \ sulfurylase)$$

$$MgATP + APS \ \square \ PAPS + MgADP \ (APS \ kinase)$$
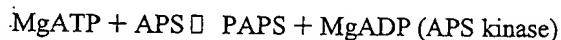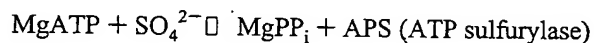
In many bacteria, yeast, and fungi, PAPS is the substrate for a reductive assimilation pathway leading to the biosynthesis of cysteine and, eventually, to all organic sulfur-containing biomolecules. Plants use APS as the activated form of sulfate for reduction. Animals do not synthesize sulfur amino acids from inorganic sulfate, but still produce PAPS that is used as the sulfuryl donor in the formation of sulfate esters.

This study focuses on APS kinase from the filamentous fungus, *Penicillium chrysogenum*, an enzyme possessing several features that make it an ideal subject for structure determination. For example, the native enzyme is a dimer composed of identical 23.67 kDa subunits (211 amino acid residues). At temperatures above ca. 42 °C, the enzyme dissociates into stable but inactive monomers. Upon cooling to □ 30 °C, the monomers reassociate forming active dimers (*1*). These observations prompt two questions. (a) What contacts stabilize the APS kinase dimer? (b) Does the active site reside at the dimer interface?

The kinetic mechanism of fungal APS kinase is compulsory ordered; MgATP adds before APS, and PAPS leaves before MgADP (*2*). The facile formation of a dead-end E·MgADP·APS complex leads to substrate inhibition by APS. The observation that APS will not bind to the free enzyme in the absence of MgATP or MgADP (*3, 4*) suggests that this obligate order is structurally based, not just a kinetic (preferred pathway) phenomenon. Another objective then was to determine whether there was any feature of the APS kinase structure that would explain the induced binding of APS.

Finally, Satishchandran et al. (*5—7*) reported that the reaction catalyzed by *Escherichia coli* APS kinase proceeded via a phosphoenzyme intermediate. The phosphoryl acceptor

* To whom correspondence should be addressed: Department of Chemistry and Section of Molecular and Cellular Biology, University of California, One Shields Avenue, Davis, CA 95616. E-mail: fisher@chem.ucdavis.edu. Phone: (530) 754-6180. Fax: (530) 752-8995.

§ Section of Molecular and Cellular Biology.
‖ Department of Chemistry.

[1] Abbreviations: APS, adenosine 5′-phosphosulfate (adenylyl sulfate); PAPS, 3′-phosphoadenosine 5′-phosphosulfate (adenylylsufate 3′-phosphate); HEPPS, N-(2-hydroxyethyl)piperazine-N′-3-propanesulfonic acid; MES, 2-(4-morpholino)ethanesulfonic acid; SDS, sodium dodecyl sulfate; DTT, dithiothreitol; ATP-γ-S, adenosine 5′-O-(3-thiotriphosphate); GMP, guanosine 5′-monophosphate; MgATP and MgADP, magnesium complexes of adenosine 5′-triphosphate and adenosine 5′-diphosphate, respectively. Such solutions contain the indicated concentration of nucleotide and a fixed 5 mM excess of $MgCl_2$ at pH 8.0.

was identified as Ser 109 (analogous to Ser 107 in the fungal enzyme). Recent mutagenesis experiments (8) eliminated Ser 107 as an obligatory phosphoryl acceptor in the *P. chrysogenum* enzyme, but chemical modification and inactivation protection studies on the Ser 107 Cys mutant suggested that residue 107 is located in the vicinity of the active site. So the third objective of this study was to obtain direct evidence bearing on the location of Ser 107.

Although the sequences of APS kinases from about 20 different sources have been reported, no structure has been presented to date. In this report, we present the structure of the free enzyme determined to 2.0 Å resolution.

EXPERIMENTAL PROCEDURES

Protein Expression and Crystallization. cDNA encoding wild-type APS kinase from *P. chrysogenum* was cloned into an *E. coli* pET vector expression system (Novagen, Madison, WI) and expressed and purified as described previously (8). After purification, the enzyme was dialyzed extensively against 10 mM Na HEPPS buffer (pH 8.0) and then concentrated by membrane filtration to 10 mg of protein/ mL. The protein (at a final concentration of $\square$ 5 mg/mL) was crystallized by hanging-drop vapor diffusion and by micro batch methods at room temperature in 0.8$\square$ 1.2 M Na$^\square$/K$^\square$ tartrate and 0.1 M Na MES (pH 6.0). Crystals of the trigonal space group $P3_121$ typically appeared overnight and often grew to 1.0 mm × 1.0 mm × 1.0 mm. These crystals had a V_M coefficient of 3.0 Å^3/Da (59% solvent) assuming one monomer per asymmetric unit and the following unit cell parameters: $a \square b \square$ 85.95 Å and $c \square$ 72.34 Å. Despite the large size of the trigonal crystals, they did not diffract X-rays beyond 2.7 Å resolution.

Addition of polyethylinimine (0.5% final concentration) to the above conditions induced APS kinase to crystallize in orthorhombic space group $C222_1$ with a V_M of 2.5 Å^3/Da (51% solvent assuming one homodimer per asymmetric unit) and the following unit cell parameters: $a \square$ 78.86 Å, $b \square$ 83.48 Å, and $c \square$ 141.95 Å. The orthorhombic crystals grew much more slowly than the trigonal forms, typically appearing only after several weeks, and often as clusters of stacked plates. However, a few large single crystals were eventually obtained and were found to diffract X-rays to significantly higher resolution than the trigonal form. The orthorhombic crystals were ultimately used to determine the final structure.

Data Collection and Phase Determination. The structure of APS kinase was first determined by MIR methods using crystals of space group $P3_121$. This crystal form was chosen for our heavy atom derivative search because of the ease with which crystals could be obtained. All heavy atom soaks were conducted at room temperature in 1.2 M Na$^\square$/K$^\square$ tartrate and 0.1 M Na MES (pH 6.0). Native and derivative data were collected on a Siemens Hi-Star area detector mounted on a Rigaku rotating anode generator. Data were processed with XDS (9) and scaled with ROTAVATA/ AGROVATA (10). Heavy atom positions were determined by inspection of difference Patterson maps and difference Fourier maps. The positions were refined and MIR phases calculated using the program PHASES (11). A 2.0 Å resolution native data set, from the orthorhombic crystal, was collected on Beamline 9-1 at SSRL and processed with DENZO and SCALEPACK (12). Table 1 lists data collection and processing statistics.

Table 1: Data Collection, Phasing, and Refinement Statistics

	native	native	phenyl-Hg	ReCl$_5$
space group	$C222_1$	$P3_121$	$P3_121$	$P3_121$
X-ray source	SSRL	CuK$\square$	CuK$\square$	CuK$\square$
wavelength (Å)	0.98	1.54	1.54	1.54
resolution (Å)	2.0	3.0	2.8	3.0
no. of reflections	109188	19508	16706	15909
no. of unique reflections	31625	6148	7469	6458
completeness (%)	98.7	96.5	94.4	99.0
$R_{merge}{}^a$ (%)	4.3	7.9	4.3	6.1
heavy atom concentration (mM)			0.5	2.0
soaking time (Days)			12	2
no. of sites (ASU)			1	1
$R_{iso}{}^b$ (%)			11.9	11.9
phasing power^c			2.71	1.47
figure of merit			0.705	

Refinement Statistics	
resolution (Å)	30.0$\square$ 2.0
no. of reflections ($|F| \square$ 0)	31625
R-factor^d	20.7
$R_{free}{}^d$ (5% data)	24.9
rms for bond distances (Å)	0.018
rms for bond angles (deg)	1.80
no. of non-hydrogen protein atoms	2800
no. of water molecules	198
no. of tartrate atoms (one molecule)	10

$^a R_{merge} \square [\Sigma_h \Sigma_i |I_h \square I_{hi}|/\Sigma_h \Sigma_i I_{hi}] \times 100$, where I_h is the mean of the I_{hi} observations of reflection h. $^b R_{iso} \square \Sigma |F_{PH} \square |F_P|/\Sigma|F_{PH}| \times 100$. ^{c} Phasing power $\square \{\Sigma_h |F_{H(calc)}|^2/\Sigma_h[|F_{PH(obs)}| \square |F_{PH(calc)}|]^2\}^{1/2}$. $^d R$-Factor and R-free $\square \Sigma||F_{obs}| \square |F_{calc}||/\Sigma|F_{obs}| \times 100$ for 95% of the recorded data (R-factor) or 5% of the data (R-free).

Model Building and Refinement. The initial solvent-flattened MIR map was used to build a partial model of a single APS kinase subunit. Model building was carried out using the molecular graphics program O (13). After several rounds of model building and refinement using TNT (14), the conventional R-factor dropped to 35% for all data recorded out to 2.9 Å resolution. This structure was then used as a search model in a 2.0 Å resolution synchrotron data set from an orthorhombic $C222_1$ crystal (see above) using the molecular replacement program AMoRe (10, 15). Two equivalent peaks were found in the rotation and translation searches that corresponded to the two copies (one homodimer) in the asymmetric unit. After a single round of rigid-body refinement, the molecular replacement solution had an R-factor of 40.6% and a correlation coefficient of 65.8 for data between 10 and 4.0 Å resolution.

The molecular replacement solution of the orthorhombic data set was used to complete all ordered regions of the APS kinase dimer. Initially, after each round of model building, the structure was refined using 95% of the data to 2.5 Å resolution with TNT (14) constraining strict noncrystallographic symmetry. Refinement lowered both the R-free (16) and R-factor at every stage and improved most of the poorly defined electron density. However, at no time was any clear density observed for residues 149$\square$ 169 in either subunit in the asymmetric unit. The structure was then refined with the simulated annealing algorithm in the program CNS (17) with high restraints placed on the noncrystallographic symmetry between the two subunits in the asymmetric unit. The resolution of the data was slowly extended with each round of refinement to a final resolution of 2.0 Å. The working and test data sets maintained the same lower-resolution

reflections upon extension. At every stage of refinement, the weight placed on the noncrystallographic symmetry restraint was reevaluated to give the lowest *R*-free value. It was observed that as the model improved, the noncrystallographic weight that gave the lowest *R*-free decreased. Once the *R*-free was less than 27%, noncrystallographic symmetry restraints were released, resulting in lower *R*-free values. Refinement was completed, resulting in a final *R*-factor of 20.7% and a final *R*-free of 24.9% for all recorded data to 2.0 Å resolution. A total of 89.1% of the residues fall within the most favored region of a Ramachandran plot, and none of the residues were in the disallowed region as determined by the program PROCHECK (*18, 19*). Final refinement statistics are listed in Table 1.

Limited Proteolysis with Trypsin. Approximately 1 mg of pure APS kinase was incubated with about 0.2 µg of trypsin in 1 mL of 50 mM Tris-HCl buffer (pH 8.0) in the absence and presence of known ligands. The reaction was quenched by addition of gel loading buffer containing SDS and DTT and the mixture boiled in a water bath. The samples were then subjected to discontinuous electrophoresis on a 20% homogeneous polyacrylamide gel (*20*).

RESULTS

Crystallographic Properties. In the absence of ligands, APS kinase crystallized into two different space groups: $P3_1$-21 and $C222_1$. The structure of the enzyme was initially determined by MIR methods to 2.9 Å resolution in the trigonal crystal form. This solution had one APS kinase monomer in the asymmetric unit. The monomer of one asymmetric unit made significant crystal contacts with the monomer in an adjacent asymmetric unit, forming an APS kinase homodimer with the dimer 2-fold symmetry axis coincident with the crystallographic 2-fold axis. The structure of APS kinase was also determined by molecular replacement (using the first model described above) in the orthorhombic crystal form. This solution had one APS kinase homodimer per asymmetric unit with the two polypeptide chains designated as A and B. The homodimers observed in the orthorhombic crystals and the trigonal crystals superimpose almost perfectly onto one another with only slight deviations due to crystal contacts. The structure of APS kinase reported here was refined against a 2.0 Å resolution data set from a single orthorhombic crystal collected at a synchrotron radiation source. The final conventional *R*-factor and *R*-free of the reported refined model are 20.7 and 24.9%, respectively. The crystallographic data and refinement statistics are summarized in Table 1. The final model consists of residues 8□ 143 and 170□ 210 of the A subunit and residues 8□ 148 and 170□ 210 of the B subunit. The remaining residues did not have clearly defined electron density with which to ascertain their position.

The average temperature factor of the A subunit is 40.4 Å². The B subunit had consistently higher temperature factors with an average of 50.4 Å². The difference in temperature factors between the two copies in the asymmetric unit can be attributed to the crystal contacts that each subunit makes. A subunits pack mostly only against the A subunits of adjacent asymmetric units, while B subunits contact mostly only other B subunits. The A subunits appear to pack tighter, making more crystal contacts than B subunits in the crystal lattice, resulting in an overall lower temperature value.
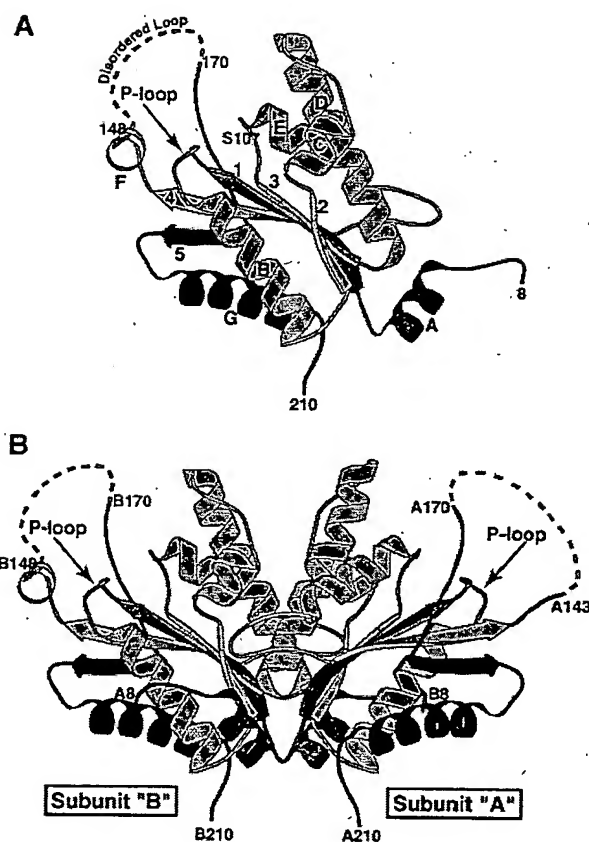

FIGURE 1: Structure of *P. chrysogenum* APS kinase. (A) The polypeptide chain of a single APS kinase subunit (as it exists in the dimer) is traced in a rainbow-colored ribbon format starting with red at the N-terminus and ending with blue at the C-terminus. The enzyme subunit is composed of a five-stranded parallel β-sheet and seven □-helices. The five strands are numbered sequentially as they occur in the primary sequence. The □-helices, which pack against the sheet, are labeled alphabetically starting with A at the N-terminus. Residues 148 and 170 delineate the ends a 21-residue stretch of the enzyme that is disordered in both subunits (dashed line). (B) APS kinase dimer. The ribbon is color-coded as described for panel A. The final model consists of residues 8□ 143 and 170□ 210 of the A subunit and residues 8□ 148 and 170□ 210 of the B subunit. Residues 143□ 149 in the B subunit (preceding the disordered loop) form one turn of an □-helix (□F), which is disordered in the A subunit. The dimer structure results in two active sites identified by their P-loops. This figure was generated using the program MOLSCRIPT (*39*).

O□erall Structure. As shown in Figure 1, the APS kinase subunit folds into a classic □/β purine nucleotide binding motif (*21*). This structure consists of an open five-stranded parallel β-sheet that is sandwiched between two □-helical bundles. In APS kinase, the β-sheet is composed mainly of hydrophobic residues that pack against predominantly hydrophobic residues of amphiphilic □-helices to form the core of each subunit. A sequence alignment of APS kinases from a variety of organisms with the secondary structure elements observed in the fungal enzyme (Figure 2) suggests that the basic structure of the enzyme is highly conserved. For the most part, deviations among species are seen only in the N- and C-termini and in the extended loops, such as the □β□ β4 loop in the fungal enzyme (residues 122□ 132), which has no counterpart in the enzyme from nonfungal sources.

Acti□e Site Region. The absence of bound substrates in the X-ray-derived structure prevents us from identifying the
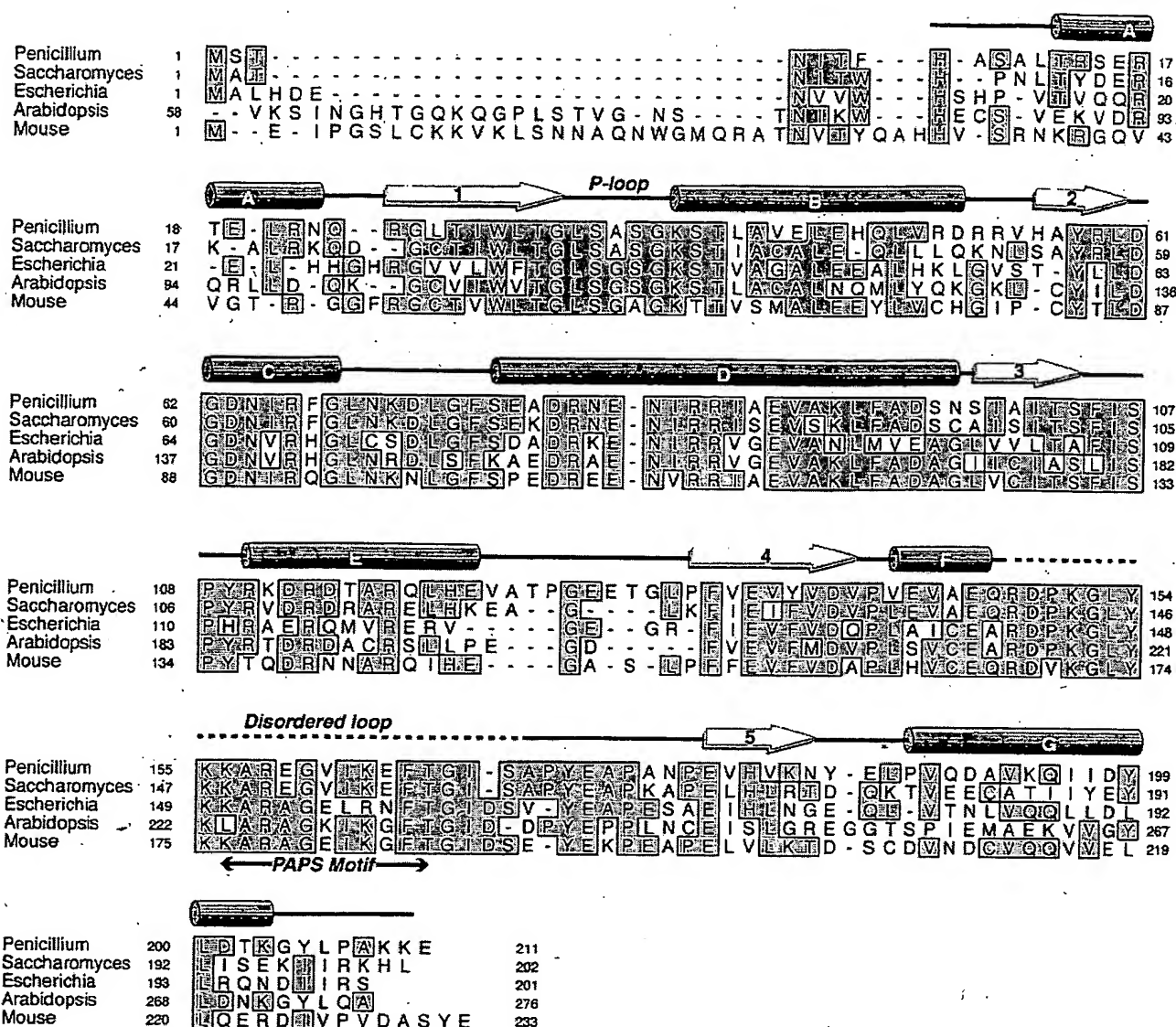
Penicillium 1 MST- N TF- - - H - ASA L RSER 17
Saccharomyces 1 MAT- N TW- - - H - - PNL YDER 16
Escherichia 1 MALHDE- NVVW- - - SHP- V TVQQR 20
Arabidopsis 58 - - VKSINGHTGQKQGPLSTVG- NS- - - - TN KW- - - HECS- VEKVDR 93
Mouse 1 M- - E- IPGSLCKKVKLSNNAQNWGMQRATNVE YQAH V- SRNKBGQV 43

P-loop

Penicillium 18 TE- RNQ- - RGL WL TGLSASGKS L AVE HQ VRDRRVHA VR D 61
Saccharomyces 17 K- A RKQD- - GCT WL TGLSASGKS I A ALE- QL LQKN SA VR D 59
Escherichia 21 - E L- HHGH GVV LWF TGLSGSGKS VAGALE A HKLGVST- VLED 63
Arabidopsis 94 QRL D- QK- - GCV WV TGL SGAGKS LA A NQM YQKGK - CV I D 136
Mouse 44 VGT- R- GG RGC V WL GLSGAGKT VSMA EY VCHGIP- CV T D 87

Penicillium 62 GDN R FGLNKDLGFSE ADRNE- N RR AEVAK FADSNS A TS F S 107
Saccharomyces 60 GDN R FGLNKDLGFSEKDRNE- N RR SEVSK FADSCA S TS F S 105
Escherichia 64 GDNVRHGLCSDLGFSDADRKE- N RRV GEVAN LMVEAG VV L A S 109
Arabidopsis 137 GDNVRHG NRDLSEKAE DRAE- N RRV GEVAK FADAG I C ASL S 182
Mouse 88 GDN RQG NKN LGFSPE DREE- NVRR AEVAK FADAG LV C TS F S 133

Penicillium 108 PYRKDRDTARQ HE VATPGEETG PFVEVYVDVPVEVAEQRDPKGLY 154
Saccharomyces 106 PYRVDRDRARELLHKEA- - G- - - - LKFIE FVDVPLEVAEQRDPKGLY 146
Escherichia 110 PHRAERQMVRERV- - - - - GE- - GR- FIEVFVDQPLAICEARDPKGLY 148
Arabidopsis 183 PYRTDRDACRSLLPE- - - GD- - - - FVEVFMDVPLSVCEARDPKGLY 221
Mouse 134 PYTQDRNNARQIHE- - - - GA- S- PFFEVFVDAP HVCEQRDVKGLY 174

Disordered loop

Penicillium 155 KKAREGV KEF TG - SAPYEAP AN EVHVKNY- E PVQDAVKQIIDY 199
Saccharomyces 147 KKAREGV KEF TG - SAPYEAPKAPELH RTD- QKTVEECATIIYEY 191
Escherichia 149 KKARAGELRNF TG DSV- YEAPESAEIHLNGE- QL- VTNLVQIQLLDL 192
Arabidopsis 222 KLARAGK KGIFTGID- DPYEPPLNCEISLGREGGTSPIEMAEKVVGY 267
Mouse 175 KKARAGEKGIFTGIDSE- YEKPEAPELVLKTD- SCDVNDCVQQVVEL 219

←PAPS Motif→

Penicillium 200 DTKGYLPAKKE 211
Saccharomyces 192 ISEK IRKHL 202
Escherichia 193 RQNDIRS 201
Arabidopsis 268 DNKGYLQA 276
Mouse 220 QERDVPVDASYE 233

FIGURE 2: Primary sequences of APS kinases from several organisms and the corresponding secondary structure of the *P. chrysogenum* enzyme. The structural elements are indicated as follows: cylinder □ □-helix, arrow □ β-strand, line □ loop or coil, and dashed line □ disordered region. The active site P-loop and the region implicated in binding (P)APS are denoted.

residues involved in catalysis by APS kinase. However, the structure of the free enzyme in combination with known sequence motifs and crystal structures of other mononucleotide kinases allows us to infer that the catalytic site lies in the vicinity of the Walker A (kinase 1a) motif, [32]GLSAS-GKS[39], which forms a characteristic P-loop structure (22□ 24). This structure, located between β1 and □B (Figure 1), has been observed in a variety of mononucleotide binding proteins, G proteins, and motor proteins, and is used to form a large "anion hole" that accommodates the phosphate groups of the nucleoside triphosphate (24□ 26).

Satischandran et al. (7) reported that Ser 109 of the *E. coli* APS kinase served as an intermediary acceptor in the overall transfer of a phosphoryl group from MgATP to APS. However, mutation of the homologous Ser 107 of the fungal enzyme to Ala or Cys did not eliminate activity, although chemical modification of the sole Cys residue in the Ser 107 Cys mutant inactivated the enzyme (8). MgATP, MgADP, or APS (in the presence of MgADP) protected the enzyme from modification and inactivation. These results suggested

that the mechanism of the fungal enzyme does not include a Ser 107 P intermediate, but that Ser 107 probably resides close to the substrate binding pocket. The crystal structure confirms this prediction. As seen in Figures 1 and 3, Ser 107 is located on the conserved loop between β3 and □E with its hydroxyl group 9 Å away from the ε-amino of P-loop Lys 38.

Prior to obtaining any structural information, we wondered whether the sequence [135]EVYVD[139] played a role in substrate binding. This stretch, which is conserved among APS kinases, is similar to the Walker B (kinase 2) motif (22, 23). In all previous structures of proteins involving P-loop-mediated binding to MgATP, the Walker B motif resides in the β-strand adjacent to the P-loop. The conserved Asp hydrogen bonds to one of the water molecules surrounding the Mg[20] of MgATP (24). In APS kinase, however, [135]EVYVD[139] is located on strand β4, which is positioned on the opposite side of the P-loop. Consequently, Asp 139 cannot interact directly with bound MgATP. Thus, [135]EVYVD[139] is unlikely to be a Walker B motif. For similar

FIGURE 3: Stereo superposition of the P-loop active site region. Shown are the active site regions from the enzymes APS kinase (red) and guanylate kinase (blue) and the 6-phosphofructo-2-kinase domain (green) of the bifunctional enzyme 6-phosphofructo-2-kinase/fructose-2,6-bisphosphatase. Also shown is the ATP-γ-S (ball-and-stick model with green bonds) as observed in the 6-phosphofructo-2-kinase domain and the GMP (ball-and-stick model with blue bonds) seen in guanylate kinase. The binding of these two substrates in their respective enzymes provides clues to the location of the substrate binding sites in APS kinase. This figure was generated using the program MOLSCRIPT (*39*) and rendered by Raster3D (*40*).

reasons, the sequence [149]DXXG[152] probably plays no role in nucleotide binding by APS kinase (Figure 1).

Superposition of the APS kinase active site region onto other P-loop-containing mononucleotide kinases, G proteins, and motor proteins revealed that Ser 104 structurally substitutes for the normally conserved aspartate of the Walker B motif found in these other proteins (Figure 3). However, these residues are not functionally equivalent. When Ser 104 was replaced with Ala, the mutant enzyme was fully active and actually had a higher affinity for APS than the wild-type enzyme (*8*). Thus, Ser 104 is not essential for substrate binding or catalysis. The X-ray structure of bovine mitochondrial F1-ATPase (*27*) may be more relevant because its Walker B Asp maps to Asp 61 of APS kinase, a residue universally conserved in all APS kinases. Asp 61 resides next to Ser 104, but in the adjacent strand (Figure 3) and, consequently, is too far removed (at least, in the free enzyme) to hydrogen bond to a water molecule surrounding the Mg^{2+}. But the APS kinase structure can accommodate slight movement around Asp 61 (the $\beta2\Box\Box C$ loop should be somewhat flexible). Such a conformational change induced by MgATP binding could position APS-binding residues in a pocket formed by helices $\Box C\Box\Box E$ (Figure 3). The Mg^{2+}-induced conformational change required for APS binding is corroborated by the observation that the APS binding affinity decreases $\Box$ 100-fold when APS kinase is bound to ADP in the absence of Mg^{2+} (*3*). The location of the putative APS binding subsite is similar to those of the acceptor substrates in adenylate kinase and guanylate kinase (*28, 29*), i.e., in other enzymes that catalyze the phosphorylation of mono-

nucleotides (Figure 3). An induced conformational change triggered by Asp 61 interacting with MgATP may also serve as the basis of the obligatory ordered binding of substrates (MgATP before APS). Attempts to diffuse MgADP alone or with APS resulted in crystal disintegration of both APS kinase crystal forms, suggesting large conformational changes upon binding substrates, subsequently disrupting vital crystal contacts.

Disordered Region. The most striking feature of the ligand-free structure is that residues 149$\Box$169 are completely disordered in both subunits. At no time during refinement was there any clear and contiguous electron density for any of the 21 residues in either subunit. The lack of order in this region was also observed in the structure determined in the trigonal space group with only one subunit per crystallographic asymmetric unit. In the B subunit, residues 142$\Box$147 form one turn of an $\Box$-helix ($\Box$F) before the electron density diminishes (in the A subunit, the last ordered residue is 143). This suggests that the first part of the disordered region may form a longer helix as is observed in the structurally homologous adenylate kinase, guanylate kinase, and thymidine kinase. In these enzymes, the region that is topologically equivalent to the APS kinase disordered region extends over the P-loop and makes contact with both the nucleoside triphosphate donor and the phosphoryl acceptor (*29$\Box$31*). Thus, it may be no coincidence that the disordered region of APS kinase contains [156]KAREGVIKEFT[166], a sequence present in several (P)APS-binding enzymes (*7*). We suggest that the high degree of flexibility in this region is not a crystallization artifact but, rather, is a reflection of
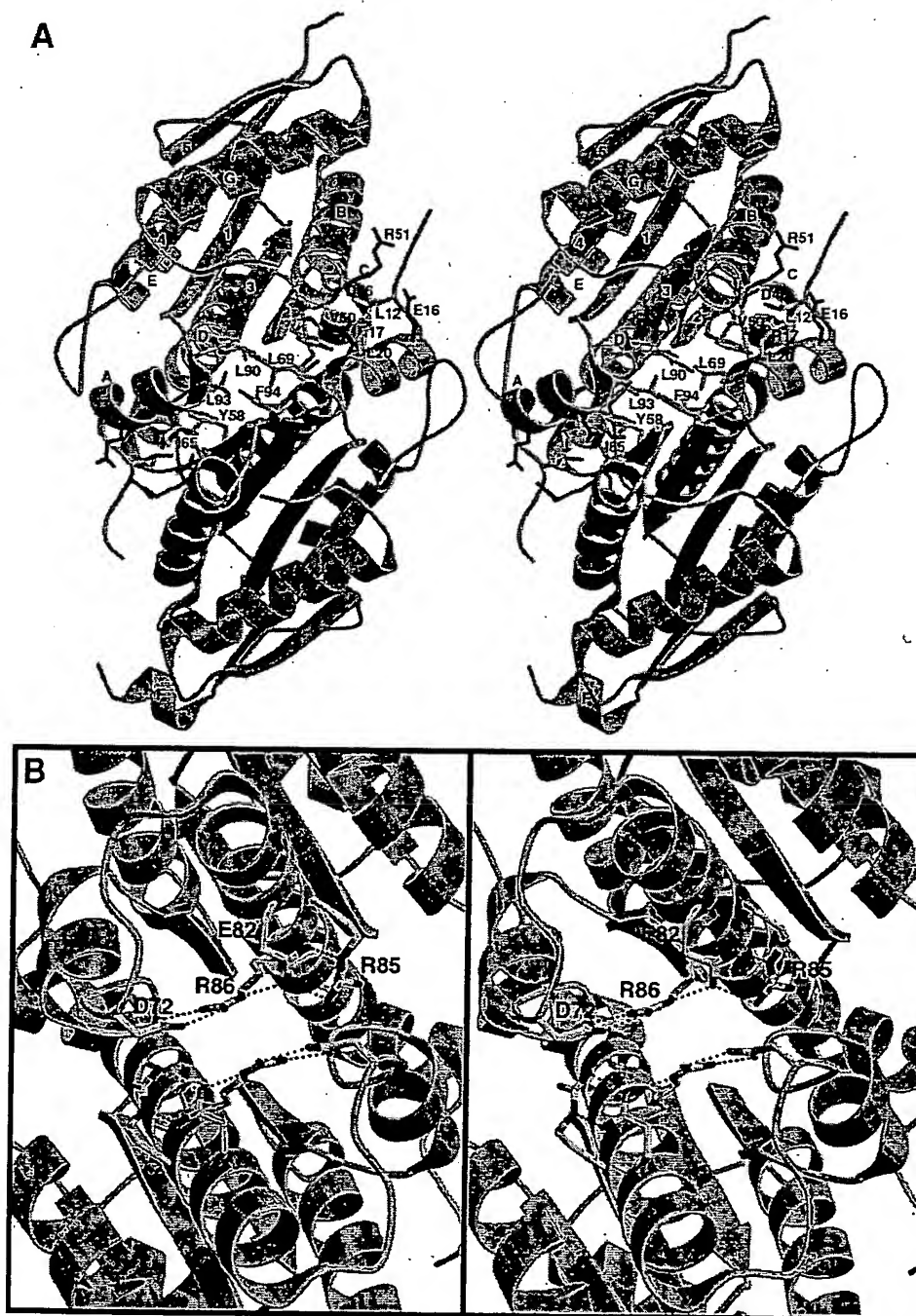
A

B

FIGURE 4: Dimer interface. (A) Stereoview of the APS kinase dimer highlighting residues that stabilize the interface. The view is looking up the dimer 2-fold axis from the "bottom". The A and B subunits are colored red and blue, respectively. The residues interacting across the dimer interface are color-coded as follows: green □ hydrophobic, red □ acidic, and blue □ basic. (B) Closeup "top" view of charged residues lying near the dimer interface that form intrasubunit salt bridges. The view is approximately down the 2-fold axis but rotated 180° around the vertical axis from the view in panel A.. These subunits have the potential to form an intersubunit salt bridging network by rotation of side chains. The A and B subunits are colored red and blue, respectively, and the charged residues in the A subunit are labeled. This figure was generated with the program MOLSCRIPT (*39*) and rendered by Raster3D (*40*).

the ordered binding mechanism. That is, this region, which may harbor part of the APS subsite, is highly disordered in the free enzyme.

APS Kinase Dimer. The crystallographic homodimer is consistent with studies on native APS kinase in solution (*1*). Although several other members of the □/β purine nucleotide binding superfamily form dimers (e.g., 6-phosphofructo-2-kinase and thymidine kinase), the APS kinase dimer interface appears to be unique. As shown in Figures 1B and 4, the

major intersubunit contacts are made between portions of □-helices C and D packing together with β-strands 2 and 3. Also, helices □ A and □ B of opposite subunits pack together.

The dimeric structure is stabilized by hydrophobic interactions and salt linkages (Figure 4). Residues Ile 65, Leu 69, Val 90, and Leu 93 in helices □ C and □ D of both subunits pack together at the dimer interface, forming a hydrophobic pocket. Phe 94 and Tyr 58 reside at the bottom of this pocket adjacent to the dimer 2-fold axis, resulting in a cluster of
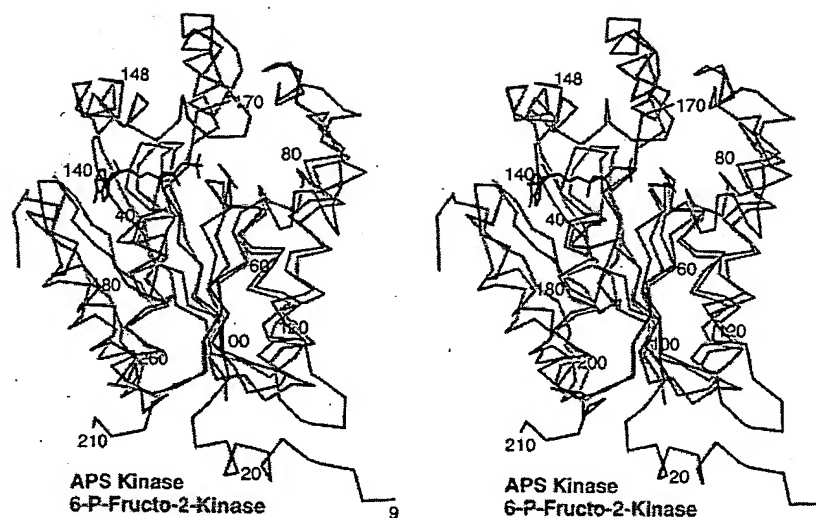
FIGURE 5: Stereoview showing the superposition of the polypeptide backbone structures of APS kinase (magenta) and the homologous 6-phosphofructo-2-kinase domain (cyan). The latter is shown with bound ATP (shown in black). The rms deviation for 131 equivalent C-α positions is 2.6 Å. This figure was generated using the program MOLSCRIPT (39).

four aromatic side chains. These four hydrophobic residues form a π stacking ladder across the interface with a distance of ~3.7 Å between the parallel aromatic side chains (Figure 4A). Other small hydrophobic pockets are made between Val 50 and Leu 12 of one subunit and Leu 20 of the other. Most of these hydrophobic residues are conserved in all APS kinases and would be solvent-exposed if the dimer were dissociated. The total buried accessible surface area at the dimer interface is 1700 Å², suggesting that there is also a good deal of van der Waals packing between the two subunits.

Although the N-terminal end of helix αD contains several charged residues that are positioned close enough to the subunit interface to make dimer-stabilizing contacts, in the free enzyme, they form intrasubunit salt bridges. Arg 85 and Asp 82 of the same subunit form a salt link, as do Arg 86 and Asp 72 (Figure 4B). All four residues lie at the N-terminal of αD near the dimer 2-fold axis, resulting in a cluster of eight charge residues that could easily salt link to residues across the dimer. These intrasubunit interactions could possibly help stabilize the monomer structure prior to dimer formation. There are only four intersubunit salt bridges in the free enzyme. These are between Glu 16 and Arg 51, and between Arg 17 and Glu 46 (Figure 4A).

It is still uncertain how the association of monomers contributes to the formation of a competent active site region. The structures shown in Figures 1 and 4 together with homology considerations (see below) eliminated one possibility, viz., that the active site resides at the subunit interface.

Structural Homologues. The C-α backbone of APS kinase was used as a search model to probe a three-dimensional structural database to find its closest relative (32). As a member of the purine nucleotide-binding superfamily of protein folds, it was expected that APS kinase would have a large number of structural homologues. The kinase domain of the bifunctional enzyme 6-phosphofructo-2-kinase/2,6-phosphofructo-2-phosphatase had the closest similarity with an rms deviation of 2.6 Å for 131 equivalent C-α positions (Figure 5). The sequences of these two proteins are only 9% identical, but the similarity in structure is not surprising. Both

enzymes catalyze the transfer of the γ-phosphoryl group from ATP to a hydroxyl group of a furanose ring sugar. By examination of these two structures, it is clear that the greatest change that occurs upon ATP binding is localized to the region corresponding to disordered residues 149–169 in APS kinase. (The disordered region of APS kinase and the corresponding region in 6-phosphofructo-2-kinase have different compositions, but are similar in length.) It has been suggested that this motion shields the bound MgATP from bulk water, thereby reducing futile ATP hydrolysis (26). The high mobility of this region is consistent with the high degree of disorder that we detected in the X-ray structure of unliganded APS kinase. The E·MgATP complex of 6-phosphofructo-2-kinase very likely provides a glimpse of what APS kinase may look like when complexed with MgATP (Figures 3 and 5).

A variety of other kinases that catalyze the phosphorylation of small molecules are also closely related structurally to APS kinase. These include deoxynucleoside monophosphate kinase (with an rms deviation of 2.9 Å for 129 C-α atoms), adenylate kinase (3.0 Å for 135 C-α atoms), guanylate kinase (3.1 Å for 126 C-α atoms), and thymadine kinase (3.5 Å for 129 C-α atoms).

Limited Proteolysis and Protection by Ligands. If, as the X-ray structure suggests, the disordered region of APS kinase is flexible and solvent-exposed, then this part of the enzyme should be highly accessible to a protease in solution. Furthermore, if the binding of MgATP or MgADP causes this region to assume a more highly structured state, then either of these nucleotides should protect this region from proteolysis.[2] Figure 6 shows the results of an experiment in which APS kinase was incubated with a small quantity of trypsin in the presence and absence of various ligands. In the absence of ligands, the enzyme is cleaved rapidly, producing a fragment that is about 5–6 kDa smaller than

---

[2] It should be noted that the proteolysis experiments were also motivated by an earlier observation that the APS kinase-like, C-terminus of fungal ATP sulfurylase is rapidly cleaved by low levels of trypsin at a position corresponding to Lys 163 in true APS kinase. This initial cleavage was followed by another at the position corresponding to Arg 117 (L. Daly, I. J. MacRae, and I. H. Segel, unpublished results).
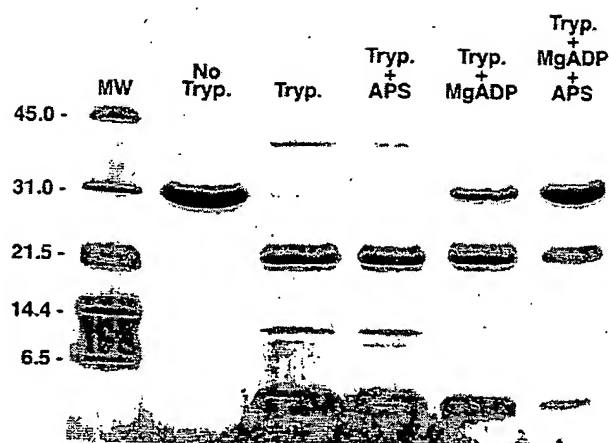
FIGURE 6: Protection against limited proteolysis of APS kinase by trypsin (Tryp.). The digestion patterns after incubation for 90 min in the presence of the indicated additions are shown. Preliminary experiments established that a 90 min digest resulted in most of the original enzyme being cleaved (data not shown). The incubation mixture contained APS kinase (1 mg/mL) and trypsin (0.2 μg/mL) in 0.05 M Tris-HCl buffer (pH 8.0). Each lane was loaded with the equivalent of 2 μg of APS kinase. MgADP and APS concentrations were 10 and 0.1 mM, respectively, when indicated. Protection by MgATP alone was identical to that provided by MgADP without APS (not shown). Molecular mass standards are shown (lane 1) with their respective mass in kilodaltons. APS kinase, whose calculated molecular mass is 23.7 kDa, runs anomalously high (lane 2). N-Terminal sequence analysis of the ~22 and ~5 kDa fragments verifies trypsin cleavage occurs at Arg 158.

the whole enzyme (Figure 6, lane 3). The size reduction is consistent with cleavage at a site somewhere between Arg 148 and Lys 163, i.e., within the disordered region. N-Terminal sequence analyses of the major band (~22 kDa) yielded STNITFHA, i.e., the N-terminal sequence of the original enzyme minus Met 1 (Figure 2). N-Terminal sequencing of the ~5 kDa cleavage product yielded EGX-IKEFT. These results confirm that the primary cleavage occurred at Arg 158 in the disordered loop and not 5□ 6 kDa in from the N-terminus. As shown in Figure 6, MgADP provided partial protection against cleavage (MgATP behaved just like MgADP; data not shown). APS alone had no effect, but augmented the protection provided by MgADP. The results are consistent with both the steady state kinetics of the APS kinase reaction (2) and various binding studies (3, 4) which show that APS binds only to the E□MgATP or E□MgADP complex.

DISCUSSION

The kinetic mechanism of *P. chrysogenum* APS kinase has been shown to be obligatory ordered; MgATP (or MgADP) adds before APS, and PAPS dissociates before MgADP (2, 33). Inactivation protection studies (3) and direct equilibrium binding studies (4) indicated that the ordered sequence was structurally based, not simply a kinetic phenomenon. For example, in the absence of MgATP or MgADP, no APS binding could be detected even at APS concentrations up to 1 mM. However, in the presence of 5 mM MgADP, APS binds with an apparent K_d of ca. 2 μM. The structure of APS kinase presented in this report supports the suggestion that structural changes underlie the ordered binding. The relevant observations are that (a) the MgATP-binding P-loop structure is well-defined. However, (b)

residues 149□ 169 are disordered in both copies of the asymmetric unit. This disordered region contains the putative APS binding sequence ([156]KAREGVIKEFT[166]) (7).

A high degree of flexibility of the disordered region is supported by protease-sensitivity studies. In the absence of any ligands, the enzyme is readily cleaved by trypsin at Arg 158. But in the presence of MgATP or MgADP, the region was protected. APS alone had no effect, but enhanced the protection provided by MgADP.

We suggest the following plausible model. The disorder of the stretch of residues 149□ 169 reflects a high degree of flexibility of this region and is responsible for the absence of a functional APS binding site on the free enzyme. MgATP binding to the P-loop concomitantly triggers (a) a displacement of Asp 61 (to stabilize the E□MgATP complex) and (b) a movement of the disordered region that results in the formation of a functional APS subsite in a pocket located between helices □ C□ □ E (Figure 3). When both substrates are bound, the (now, highly ordered) stretch of residues 149□ 169 behaves as a lid to cover the active site. The lid itself may contain residues that bind APS, thereby contributing to the stability of the ternary E□MgATP□APS complex. This scenario is reminiscent of the domain-closure mechanism observed in substrate binding to adenylate kinase (30). The structural changes proposed for the fungal enzyme, however, may not be able to be applied to APS kinases from all sources. For example, the *E. coli* enzyme is reported to bind APS in the absence of MgATP (5, 6).

In animals, ATP sulfurylase and APS kinase reside on a single (bifunctional) polypeptide chain with a structure that has been described schematically as [1]APS□ kinase[199]□ [200]linker[236]□ [237]ATP□ sulfurylase[624] (34). Deyrup et al. reported that the expressed bifunctional mouse protein displayed no significant APS kinase activity (a) if the kinase domain (APSK) was expressed independently of the downstream "linker" and sulfurylase (ATPS) domains, (b) if the kinase and sulfurylase domains were joined without the "linker" region, or (c) if the two domains were rearranged without the "linker" (i.e., ATPS□ APSK). The latter construct resembles the fungal ATP sulfurylase (35), except that in the fungal protein, the APS kinase-like domain has no kinase activity; it serves solely as an allosteric domain for binding PAPS (36). If the structure of mouse APS kinase in the region of residues 200□ 230 is similar to that of the fungal enzyme (in the corresponding stretch of residues 180□ 211), then the absence of APS kinase activity in the constructs of the mouse enzyme lacking residues 200 to ca. 230 is not unexpected. That region may not be a linker but, rather, an integral part of the enzyme that is homologous to strand $\beta5$, and helix □ G of the fungal enzyme. Examination of 16 published sequences of APS kinases shows only a low level of identity in this region, but a degree of similarity suggesting that this region is an important part of the enzyme from all sources.

APS kinase from *P. chrysogenum* contains no sulfur amino acids except for the N-terminal Met. Plant APS kinases, on the other hand, contain from four to eight Cys residues per subunit. A sulfhydryl□ disulfide interconversion (37) mediated by thioredoxin (38) may regulate APS kinase in plants. If this is the case, the structure of *P. chrysogenum* APS kinase suggests that the Cys residues involved in this redox process are Cys 132 and Cys 176. These are the only two Cys residues close enough together in *Arabidopsis* APS kinase

to form an intrasubunit disulfide bond. (The □-carbons are 5.8 Å apart. All others are □ 10 Å apart.)

REFERENCES

1. Renosto, F., Seubert, P. A., Knudson, P., and Segel, I. H. (1985) *J. Biol. Chem. 260*, 15350 1544.
2. Renosto, F., Seubert, P. A., and Segel, I. H. (1984) *J. Biol. Chem. 259*, 21113 2123.
3. Renosto, F., Seubert, P. A., Knudson, P., and Segel, I. H. (1985) *J. Biol. Chem. 260*, 119030 11913.
4. Renosto, F., Martin, R. L., and Segel, I. H. (1991) *Arch. Biochem. Biophys. 284*, 300 34.
5. Satishchandran, C., and Markham, G. D. (1989) *J. Biol. Chem. 264*, 150120 15021.
6. Satishchandran, C., and Markham, G. D. (1990) *FASEB J. 4*, A2119 (abstract 2467).
7. Satishchandran, C., Hickman, Y. N., and Markham, G. D. (1992) *Biochemistry 31*, 116840 11688.
8. MacRae, I., Rose, A. B., and Segel, I. H. (1998) *J. Biol. Chem. 273*, 285830 28589.
9. Kabsch, W. (1988) *J. Appl. Crystallogr. 21*, 9160 924.
10. Collaborative Computational Project 4 (1994) *Acta Crystallogr. D50*, 7600 763.
11. Furey, W., and Swaminathan, S. (1997) *Methods Enzymol. 277*, 5900 620.
12. Otwinowski, Z., and Minor, W. (1997) in *Methods in Enzymology* (Carter, C. W., Jr., and Sweet, R. M., Eds.) pp 3070 326, Academic Press, New York.
13. Jones, T. A., Zou, J. Y., Cowan, S. W., and Kjeldgaard, M. (1991) *Acta Crystallogr. A47*, 1100 119.
14. Tronrud, D. E., Ten-Eyck, L. F., and Matthews, B. W. (1987) *Acta Crystallogr. A43*, 4890 501.
15. Navaza, J. (1993) *Acta Crystallogr. D49*, 5880 591.
16. Brünger, A. T. (1993) *Acta Crystallogr. D49*, 240 36.
17. Brünger, A. T., Adams, P. D., Clore, G. M., DeLano, W. L., Gros, P., Grosse-Kunstleve, R. W., Jiang, J.-S., Kuszewski, J., Nilges, M., Pannu, N. S., Read, R. J., Rice, L. M., Simonson, T., and Warren, G. L. (1998) *Acta Crystallogr. D54*, 9050 921.
18. Laskowski, R. A., MacArthur, M. W., Moss, D. S., and Thornton, J. M. (1993) *J. Appl. Crystallogr. 26*, 2830 291.
19. Ramakrishnan, C., and Ramachandran, G. N. (1965) *Biophys. J. 5*, 9090 933.
20. Laemmli, U. K. (1970) *Nature 227*, 6800 685.
21. Schulz, G. E., and Schirmer, R. H. (1974) *Nature 250*, 1420 144.
22. Walker, J. E., Saraste, M., Runswick, M. J., and Gay, N. J. (1982) *EMBO J. 1*, 9450 951.
23. Traut, T. W. (1994) *Eur. J. Biochem. 222*, 90 19.
24. Smith, C. A., and Rayment, I. (1996) *Biophys. J. 70*, 15900 1602.
25. Dreusicke, D., and Schultz, G. E. (1986) *FEBS Lett. 208*, 3010 304.
26. Schulz, G. E. (1992) *Curr. Opin. Struct. Biol. 2*, 610 67.
27. Abrahams, J. P., Leslie, A. G., Lutter, R., and Walker, J. E. (1994) *Nature 370*, 6210 628.
28. Abele, U., and Schulz, G. E. (1995) *Protein Sci. 4*, 12620 1271.
29. Stehle, T., and Schulz, G. E. (1992) *J. Mol. Biol. 224*, 11270 1141.
30. Schlauderer, G. J., Proba, K., and Schulz, G. E. (1996) *J. Mol. Biol. 256*, 2230 227.
31. Wild, K., Bohner, T., Folkers, G., and Schulz, G. E. (1997) *Protein Sci. 6*, 20970 2106.
32. Holm, L., and Sander, C. (1993) *J. Mol. Biol. 233*, 1230 138.
33. MacRae, I. J., and Segel, I. H. (1999) *Arch. Biochem. Biophys. 361*, 2770 282.
34. Deyrup, A. T., Krishnan, S., Singh, B., and Schwartz, N. B. (1999) *J. Biol. Chem. 274*, 107510 10757.
35. Foster, B. A., Thomas, S. M., Mahr, J. A., Renosto, F., Patel, H., and Segel, I. H. (1994) *J. Biol. Chem. 269*, 197770 19786.
36. Renosto, F., Martin, R. L., Wailes, L. M., Daley, L. A., and Segel, I. H. (1990) *J. Biol. Chem. 265*, 103000 10308.
37. Jender, H. G., and Schwenn, J. D. (1984) *Arch. Microbiol. 138*, 90 14.
38. Schwenn, J. D., and Schriek, U. (1984) *FEBS Lett. 170*, 760 80.
39. Kraulis, P. J. (1991) *J. Appl. Crystallogr. 24*, 9460 950.
40. Merritt, E. A., and Murphy, M. E. P. (1994) *Acta Crystallogr. D50*, 8690 873.

BI9924157